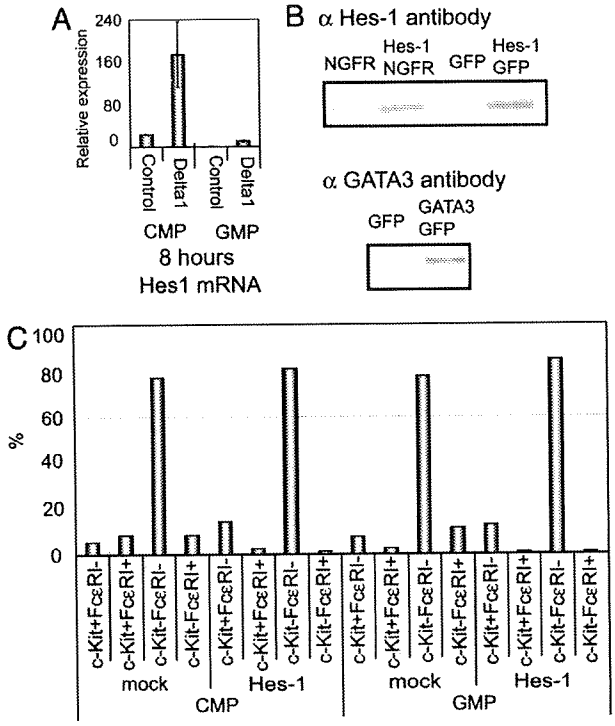

Fig. 2. Hes-1 up-regulation downstream of Notch signaling is insufficient for mast cell derivation. (*A*) CMPs and GMPs were stimulated with plate-fixed Delta1-Fc protein or control Fc protein in SCF, IL-3, IL-6, and TPO. Cells were collected at 8 h, and Hes-1 mRNA was measured by quantitative real-time PCR analysis. Hes-1 mRNA was substantially up-regulated with Delta1-Fc compared with control. Data are presented as mean +/− SD; $n = 4$, $P = 0.0286$ (both CMPs and GMPs, 8 h) (nonparametric test). (*B*) A retrovirus packaging cell line, PLAT-E, was transfected with cDNA-subcloned retrovirus vectors, i.e., Hes-1-GCDNsam/IRES-NGFR, Hes-1-pMYs/IRES-GFP, and GATA3-pMYs/IRES-GFP, or a mock retrovirus vector. NIH 3T3 cells were infected with the conditioned medium by using polybrene. The proteins were detected by anti-Hes-1 antibody (H-140; Santa Cruz) and anti-GATA3 antibody (HG3–31). There is a faint band migrating in the NGRF and GFP lanes. This may represent endogenously expressed Hes-1. (*C*) CMPs and GMPs were retrovirally transduced with Hes-1-pMYs/IRES-GFP or mock virus. The proportion of c-Kit$^+$FcεRI$^+$ mast cells was not significantly increased by Hes-1 expression. The proportion of c-Kit$^+$FcεRI$^-$ cells, which probably represent myeloid progenitors, was always greater in the Hes-1-expressing population than control.

regulated during Notch-mediated inhibition of granulocytic differentiation (12, 13), is proposed to be a regulator of mast cell differentiation (4, 5, 14). Nevertheless, GATA2 expression levels in CMPs or GMPs stimulated with Delta1-Fc were equal to or lower than those stimulated with control Fc protein during the first 48 h (Fig. 3*A*).

GATA3 is a crucial transcription factor during T cell development. Recently, it was reported that its overexpression in double negative (DN) 1 and DN2 stage thymocytes blocked further T cell development, and unexpectedly, induced mast cells from these early thymocyte populations (15). Physiologic relevance between GATA3 and mast cell generation, however, has yet to be elucidated. Delta1-Fc stimulation of CMPs and GMPs substantially increased GATA3 mRNA during a relatively later time course (Fig. 3*B*). This finding suggests that GATA3 is a possible target of Notch signaling, albeit indirect, for mast cell production.

Thus, we examined whether Hes-1 and GATA3 are bona fide effectors functioning downstream of Notch signaling for mast cell production, by retrovirally transducing CMPs and GMPs with these genes (Fig. 3 *C* and *D*). Both CMP- and GMP-derived fractions expressing Hes-1 alone [with the nerve growth factor receptor (NGFR) marker] gave rise to populations very similar to those derived from the fraction expressing Hes-1 with the GFP marker (Figs. 2*C* and 3 *C* and *D*). There was no consistent increase in the c-Kit$^+$FcεRI$^+$ mast cell population at day 8, although it appears that the Hes-1 single-positive CMP-derived fraction gave rise to this population slightly more than control in Fig. 3 *C* and *D*. On the contrary, the Hes-1 single-positive fractions gave rise to fewer mast cells than the control virus-infected fractions at the later time course (data not shown). In the fractions expressing GATA3 alone (with the GFP marker), the c-Kit$^+$FcεRI$^+$ mast cell population only marginally, although reproducibly, increased compared with controls (Fig. 3 *C* and *D*).

In contrast to these findings, the c-Kit$^+$FcεRI$^+$ mast cell population was markedly enriched in the Hes-1 and GATA3 double-positive fractions at day 8 after the infection of CMPs and GMPs compared with either mock or Hes-1 or GATA3 single-positive fractions (Fig. 3 *C* and *D*).

We reproducibly observed increases in the c-Kit$^+$FcεRI$^-$ population, which might represent the expanded progenitors maintaining the immature state, in the Hes-1 single-positive fractions. The c-Kit$^-$FcεRI$^+$ population, whose identification is unknown, variably increased in the GATA3 single-positive fractions compared with controls (Fig. 3*C*).

When plated in methylcellulose after the retroviral infection, Hes-1- and GATA3-coexpressing CMPs and GMPs formed large and monotonous cell-containing colonies (plating efficiency, ≈20% in CMPs and <10% in GMPs); staining indicated that >80% of colonies contained mast cells, positive for toluidine blue, as the major population (Fig. 3 *E–G*), whereas the plating efficiency was comparable to that with mock introduction (Fig. 3*E*).

These observations indicate that the simultaneous expression of GATA3 and Hes-1 biased the cell fate of myeloid progenitors toward the downstream progenitors having mast cell-generating capacity at the single-cell level, rather than that those transcription factors expanded the pool of mast cell progenitors or mast cells.

Hes-1 Up-Regulation Causes C/EBPα Down-Regulation. C/EBPα is a critical transcription factor for myeloid differentiation (16), and its down-regulation cooperates with the up-regulation of a GATA transcription factor to instruct mast cell development (5). At 48 h after the initiation of Hes-1 retroviral transduction, C/EBPα mRNA was down-regulated in both CMPs and GMPs (Fig. 4*A*). The C/EBPα mRNA level was also markedly suppressed in a mouse myeloid cell line 32D that stably expressed exogenous Hes-1 (Fig. 4*B*). These findings suggest that the C/EBPα down-regulation is the major outcome of Hes-1 up-regulation induced by Delta1–Notch2 signaling in the myeloid progenitors.

Discussion

In the present study, we demonstrate that Notch2-mediated signaling has a significant role in the mast cell derivation from myeloid progenitors such as CMPs and GMPs. This biological effect is probably mediated through coordinated up-regulation of Hes-1 and GATA3 through Notch2 signaling; Hes-1 up-regulation further results in C/EBPα down-regulation, which is important for the blockade of myeloid lineage differentiation. It is not unexpected that Hes-1 up-regulation plays a role in the execution of Notch2 signaling, given the fact that Hes-1 is an established target of Notch signaling in a number of cell systems (17). However, we show in this article that Hes-1 up-regulation represents only a part of signaling downstream of Notch activation. Exogenous Hes-1 expression in CMPs and GMPs resulted in the increase of Lin$^-$c-Kit$^+$FcεRI$^-$ cells, obviously different

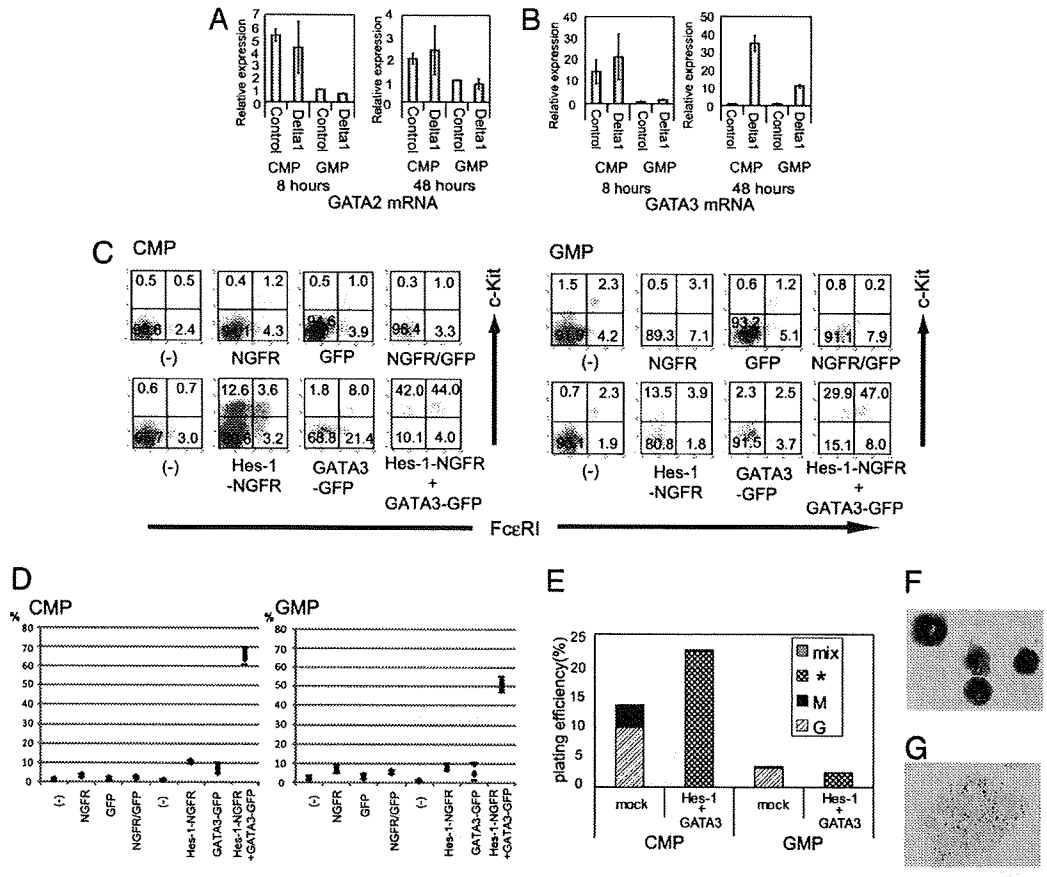

Fig. 3. GATA3, but not GATA2, is a mediator downstream of Notch2 for mast cell developmental decision, together with Hes-1. (*A*) CMPs and GMPs were stimulated with plate-fixed Delta1-Fc in the presence of SCF, IL-3, IL-6, and TPO for 8 or 48 h. Cells were harvested, and quantitative real-time PCR was performed. GATA2 mRNA levels were slightly decreased rather than increased by Delta1-Fc in GMPs at 8 h, and not significantly different in CMPs treated with Delta1-Fc and control Fc at 8 h or in CMPs and GMPs treated with Delta1-Fc and control Fc at 48 h. (*B*) Quantitative real-time PCR analyses in CMPs and GMPs revealed that GATA3 mRNA was up-regulated by Delta1-Fc at 48 h, but not at 8 h. Data are presented as mean +/− SD; $n = 4$, $P = 0.6857$ (CMPs, 8 h); $n = 4$, $P = 0.0571$ (GMPs, 8 h); $n = 4$, $P = 0.0286$ (both CMPs and GMPs, 48 h) (nonparametric test). (*C*) CMPs and GMPs were retrovirally transduced with Hes-1-GCDNsam/IRES-NGFR and GATA3-pMYs/IRES-GFP and subjected to FACS analysis 8 days after the infection. The c-Kit$^+$FcεRI$^+$ fraction was remarkably enriched in Hes-1 and GATA3 double-positive fraction compared with the Hes-1 or GATA3 single-positive fraction or the mock virus-introduced fraction. (*D*) The proportions of c-Kit$^+$FcεRI$^+$ fraction are depicted. Each diamond represents a data point. The bars represent +/− 2 SD. CMP, $n = 6$; GMP, $n = 4$. (*E*) NGFR and GFP double-positive cells were sorted at 48 h after infection. Two hundred and fifty NGFR and GFP double-positive CMPs and 1,500 GMPs were plated per dish and cultured for 7 days in methylcellulose, supplemented with SCF, IL-3, IL-6, and TPO. Hes-1- and GATA3-coexpressing cells formed mainly mast cell colonies, whereas mock virus-transduced cells formed various colonies including granulocyte, macrophage, or a mixture of these cells. G, granulocyte colonies; M, macrophage colonies; mix, granulocyte/macrophage or mixed colonies; *, colonies mainly consisting of mast cells. The result of a representative experiment is shown ($n = 2$). (*F*) Wright-Giemsa staining of Hes-1 and GATA3 coexpressing colony-forming cells. (Original magnification: ×400.) (*G*) Toluidine blue staining of Hes-1 and GATA3 coexpressing colony-forming cells. (Original magnification: ×400.)

from the Lin$^-$c-Kit$^+$FcεRI$^+$ mast cell enrichment that was seen by the Delta1 stimulation. Although the identity of the Lin$^-$c-Kit$^+$FcεRI$^-$ cells has yet to be determined, these cells may contain immature myeloid progenitors that could differentiate into mast cells if GATA3 would coexist, while granulocytes/macrophages would if other critical molecules (such as C/EBPα) would coexist.

We identified GATA3, not GATA2, up-regulation that complements Hes-1 up-regulation and creates a part of Notch signaling. Involvement of GATA2 is proposed to be important for inhibiting granulocytic differentiation downstream of Notch signaling in both the 32D cell line (13) and mouse hematopoietic progenitor cells (12). Furthermore, GATA2 is required for *in vitro* mast cell generation (4, 14), and enforced expression of GATA2 instructs the C/EBPα-deficient myeloid progenitors and common lymphoid progenitors to become mast cells *in vitro* (5). Our conclusion might appear to be inconsistent with those of other articles. We confirmed that the enforced GATA2 and Hes-1 coexpression in CMPs and GMPs resulted in predominant mast cell generation in a manner indistinguishable from that of GATA3 and Hes-1 coexpression (data not shown). This finding indicates that GATA2 and GATA3 have redundant properties when they are expressed exogenously. The result of colony formation assay from CMPs and GMPs with enforced GATA3 and Hes-1 expression indicates that the mast cell derivation is based on the cell fate alteration made in the individual progenitor cells. Because the biological readout for Notch ligand stimulation was virtually the same as that for the GATA3 and Hes-1 coexpression, the substantial mast cell generation at day 7 with Delta1-Fc is likely to be caused mainly by biased cell fate decision in the myeloid progenitors.

In a different line, the introduction of GATA3 alone to thymocytes was recently reported to result in mast cell generation (15). Although this report might appear to be inconsistent

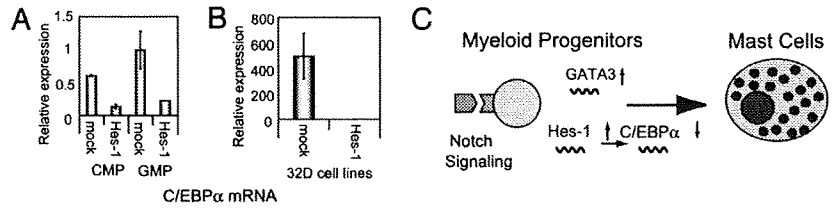

Fig. 4. Hes-1 up-regulation causes C/EBPα down-regulation. (*A*) CMPs and GMPs were retrovirally transduced with Hes-1-pMYs/IRES-GFP. GFP$^+$ cells were sorted 48 h after infection and examined for C/EBPα mRNA by quantitative real-time PCR. C/EBPα mRNA in CMPs and GMPs was substantially reduced by Hes-1 compared with mock virus transduction. Data are presented as mean +/− SD; $n = 5$ (mock) or 4 (Hes-1), $P = 0.0159$ (CMP); $n = 5$, $P = 0.0079$ (GMP) (nonparametric test). (*B*) 32D cells stably transduced with Hes-1 and maintained in 5 ng/ml IL-3 were examined for C/EBPα expression. C/EBPα mRNA was reduced in Hes-1-transduced clones compared with mock-transduced clones. Data were confirmed by experiments using two independent clones. Data are presented as mean +/− SD. (*C*) Schematic model of Notch signaling in the mast cell system.

with our data, the difference in the starting cell populations could cause the different results. We conclude that the Hes-1 expression, and probably subsequent C/EBPα down-regulation, is required, although not sufficient, for mast cell generation from CMPs and GMPs. In contrast, C/EBPα is already down-regulated in thymocytes at the DN1 and DN2 stages (18), and thus, introduction of GATA3 might be sufficient for mast cell generation from early thymocytes. As for the relationship between GATA3 and Notch signaling, both Notch1 and Notch2 are important for the generation of Th2 cells and act by directly inducing transcription of GATA3 and IL-4 (19, 20). It is, however, unclear whether such a direct regulation is applicable to cells in other lineages. In our observation, GATA3 was up-regulated by Delta1-Fc at 48 h but not at 8 h in CMPs and GMPs, making it obscure whether GATA3 is a direct target of Notch signaling in these cells. The role of IL-4 in the regulation of GATA3 in these cells remains to be determined.

We and others previously reported that enforced expression of Hes-1 in a 32D cell line inhibits granulocytic differentiation induced by granulocyte colony-stimulating factor (13, 21). In the present study, we demonstrated that C/EBPα down-regulation occurs downstream of Hes-1 in both the 32D cell line and fresh CMPs and GMPs. C/EBPα repression by Hes-1 was previously shown to be among the mechanisms of Notch-Hes-1-mediated inhibition of adipogenesis from a preadipocyte cell line (22). Although less remarkable compared with Hes-1 overexpression, Delta1-Fc stimulation also induced C/EBPα repression, in a time course after Hes-1 up-regulation. This finding suggests that the physiologic Hes-1 up-regulation is sufficient for C/EBPα repression (data not shown). Our data, thus, support a paradigm that the Notch-Hes-1-C/EBPα axis consists of a common pathway for differentiation inhibition in a variety of cell lineages.

It was recently suggested that down-regulation of C/EBPα followed by up-regulation of a GATA factor orchestrates mast cell differentiation from myeloid progenitors (5). This could be true, but importantly, we demonstrated that such a balanced regulation of transcription factors is a result of environmental signaling through Notch2, rather than a cell-autonomous operation (Fig. 4*C*).

The physiological significance of Notch2-mediated cell fate bias toward mast cell lineage remains to be determined, because mast cells were not depleted in naïve status in N2-MxcKO mice (M.S.-Y. and S.C., unpublished data). Cultured mast cells were also generated from Notch2-null bone marrow cells as efficiently as WT bone marrow cells. Notably, mast cells are not depleted in mice lacking the IL-3 gene, whereas IL-3 is the most potent mast cell developmental factor *in vitro*. However, IL-3-deficient mice are defective in mast cell-mediated intestinal nematode eradication. The pathways and mechanisms responsible for regulating mast cell progenitor recruitment and trafficking are likely to be dynamic and susceptible to modification during inflammation (1). Similarly, Notch2 is required for the proper response of mast cells during nematode infection (M.S.-Y. and S.C., unpublished observation). Notch2-mediated mast cell derivation might also be required for such pathological settings, whereas it is unnecessary for the steady-state mast cell generation.

Materials and Methods

Mice. *Notch2*$^{flox/flox}$ mice have been described (10). Mx-Cre transgenic mice (23) were crossed with *Notch2*$^{flox/flox}$ mice, and the progeny were injected with pIpC (Sigma-Aldrich) seven times every other day from 3 d after birth (25 μg/g body weight) or three times between 4 and 6 wk of age (20 μg/g body weight). All experiments were done in accordance with institutional guidelines.

Myeloid Progenitors. Bone marrow cells from each mouse strain studied were incubated with biotinylated antibodies for lineage markers including anti-CD3, anti-CD4, anti-CD8, anti-B220, anti-Ter119, and anti-Gr-1 antibodies (BD Pharmingen) followed by incubation with streptavidin Micro Beads (Miltenyi Biotec). The lineage marker-negative fraction was separated with an autoMACS separator (Miltenyi Biotec) and incubated with anti-CD34-FITC, anti-CD16/32 (FcγIII/II receptor)-phycoerythrin (PE), anti-c-Kit-allophycocyanin (APC), streptavidin peridinin chlorophyll protein PerCP (BD Pharmingen), and anti-ScaI-PE/Cy7 (eBioscience). Lin$^-$c-Kit$^+$ScaI$^-$FcγR^{lo}CD34$^+$ and Lin-c-Kit$^+$ScaI$^-$FcγR^{hi}CD34$^+$ cells (CMPs and GMPs, respectively) (24) were sorted by a FACSAria cell sorter (Becton Dickinson).

Ligand Fixation. Delta1-Fc has been described (25). A 24-well nontissue culture plate (Nalge Nunc) was coated with 10 μg/ml of rabbit anti-human IgG (DAKO), blocked with 20% FBS containing RPMI medium 1640 (Sigma-Aldrich), and washed with PBS. The Delta1-Fc (3.5 μg/ml) or Fc portion of human IgG (2 μg/ml, Fc protein; ART or Jackson ImmunoResearch Laboratories) was then incubated for 30 min, and supernatants were removed.

Ligand Stimulation of Myeloid Progenitors. Sorted CMPs or GMPs were cultured in Delta1-Fc or control Fc protein-fixed plates in 20% FBS containing Iscove's modified Dulbecco's medium (Sigma-Aldrich), supplemented with 50 ng/ml SCF, 20 ng/ml IL-3 (Peprotech), 20 ng/ml IL-6, and 20 ng/ml TPO (gifts from Kirin Pharma, Tokyo). On day 7, the cells were incubated with purified isotype IgE (BD Pharmingen) after blocking the Fcγ receptor with anti-CD16/32 (Fcγ III/II receptor) antibody, stained with anti-IgE-FITC, anti-Gr-1-PE, anti-Mac1-PE, and anti-c-Kit-APC (BD Pharmingen), and then analyzed by FACSCalibur (Becton Dickinson). Cells cultured for 7 days were also characterized by Wright-Giemsa staining or toluidine blue staining (pH 0.5) on cytospin slides. In some experiments, mRNA was prepared at the indicated time points and quantified by real-time PCR as described below.

Retroviral Transduction. Hes-1 cDNA, a gift from R. Kageyama (Kyoto University, Kyoto, Japan), was subcloned into a retrovirus vector, GCDNsam/internal ribosome entry site (IRES)-NGFR, a gift from H. Nakauchi (University of Tokyo) and M. Onodera (National Center for Child Health and Development, Tokyo). cDNAs for GATA3, a gift from S. Takahashi (University of Tsukuba), and Hes-1 were subcloned into pMYs/IRES-GFP, a gift from T. Kitamura (University of Tokyo). A retrovirus packaging cell line, PLAT-E (26), was transfected with each retrovirus vector by using FuGENE 6 (Roche Diagnostics). The conditioned medium was concentrated, placed in a 24-well nontissue culture dish for 4 h, and precoated with 40 μg/ml of RetroNectin (Takara Bio) overnight at 4°C. CMPs or GMPs were then plated for infection in the presence of 20% FBS, 50 ng/ml SCF, 20 ng/ml IL-3, 20 ng/ml IL-6, and 20 ng/ml TPO. Green fluorescent

proteins and/or human NGFR-positive fractions were subjected to FACS analysis 8 days after infection. Otherwise, the infected cells were sorted at 48 h from the initiation of infection with a FACSAria (Becton-Dickinson) cell sorter and used for colony assay using Methocult M3231 (StemCell Technologies), supplemented with cytokines as described above. Hes-1 stably expressing 32D cell lines were as described (13). To confirm protein expression, NIH 3T3 cells were also infected with the same viral supernatants by using polybrene (Sigma-Aldrich).

RNA Quantitation. Total cellular RNA was extracted with RNeasy (Qiagen) and converted to cDNA with SuperScript III (Invitrogen). GATA2, GATA3, C/EBPα, and mouse mast cell protease-5 were analyzed with *Taq*Man Gene Expression assays (Applied Biosystems). Hes-1 mRNA was measured as described (10). Real-time PCR was performed by using the ABI PRISM 7000 Sequence Detection System (Applied Biosystems). All of the data were standardized with 18s ribosomal RNA.

Western Blot Analysis. Virus-infected NIH 3T3 cells were solubilized in lysis buffer containing 1% Triton X-100. The Hes-1 and GATA3 proteins were detected by anti-Hes-1 antibody (H-140; Santa Cruz) and anti-GATA3 antibody (HG3–31), respectively.

Statistical Analysis. Results from two or three independent experiments (n = 2) of quantitative real-time PCR were analyzed by the Mann–Whitney test.

ACKNOWLEDGMENTS. We thank Dr. R. Kageyama for the Hes-1 cDNA; Dr. S. Takahashi for the GATA3 cDNA; Drs. H. Nakauchi and M. Onodera for the GCDNsam/IRES-NGFR; Dr. T. Kitamura for the pMYs/IRES-GFP and PLAT-E; Kirin Pharma for the TPO and IL-6; and Y. Mori for technical assistance. This work was supported in part by Grants-in-Aid for Scientific Research Grants 18013012, 19390258 (to S.C.), and 19890051 (to M.S.-Y.) from the Japan Society for the Promotion of Science/Ministry of Education, Culture, Sports, Science, and Technology of Japan, and a grant from the Sagawa Foundation for Promotion of Cancer Research (to S.C.).

1. Gurish M-F, Boyce J-A (2006) Mast cells: Ontogeny, homing, and recruitment of a unique innate effector cell. *J Allergy Clin Immunol* 117:1285–1291.
2. Galli S-J, Nakae S, Tsai M (2005) Mast cells in the development of adaptive immune responses. *Nat Immunol* 6:135–142.
3. Shelburne C-P, *et al.* (2002) Stat5: An essential regulator of mast cell biology. *Mol Immunol* 38:1187–1191.
4. Walsh J-C, *et al.* (2002) Cooperative and antagonistic interplay between PU.1 and GATA-2 in the specification of myeloid cell fates. *Immunity* 17:665–676.
5. Iwasaki H, *et al.* (2006) The order of expression of transcription factors directs hierarchical specification of hematopoietic lineages. *Genes Dev* 20:3010–3021.
6. Radtke F, Wilson A, Mancini S-J, MacDonald H-R (2004) Notch regulation of lymphocyte development and function. *Nat Immunol* 5:247–253.
7. Tsukumo S, Yasutomo K (2004) Notch governing mature T cell differentiation. *J Immunol* 173:7109–7113.
8. Singh N, Phillips R-A, Iscove N-N, Egan S-E (2000) Expression of notch receptors, notch ligands, and fringe genes in hematopoiesis. *Exp Hematol* 28:527–534.
9. Jonsson J-I, Xiang Z, Pettersson M, Lardelli M, Nilsson G (2001) Distinct and regulated expression of Notch receptors in hematopoietic lineages and during myeloid differentiation. *Eur J Immunol* 31:3240–3247.
10. Saito T, *et al.* (2003) Notch2 is preferentially expressed in mature B cells and indispensable for marginal zone B lineage development. *Immunity* 18:675–685.
11. Jarriault S, *et al.* (1995) Signaling downstream of activated mammalian Notch. *Nature* 377:355–358.
12. de Pooter R-F, *et al.* (2006) Notch signaling requires GATA-2 to inhibit myelopoiesis from embryonic stem cells and primary hemopoietic progenitors. *J Immunol* 176:5267–5275.
13. Kumano K, *et al.* (2001) Notch1 inhibits differentiation of hematopoietic cells by sustaining GATA-2 expression. *Blood* 98:3283–3289.
14. Tsai F-Y, Orkin S-H (1997) Transcription factor GATA-2 is required for proliferation/survival of early hematopoietic cells and mast cell formation, but not for erythroid and myeloid terminal differentiation. *Blood* 89:3636–3643.
15. Taghon T, Yui M-A, Rothenberg E-V (2007) Mast cell lineage diversion of T lineage precursors by the essential T cell transcription factor GATA-3. *Nat Immunol* 8:845–855.
16. Zhang P, *et al.* (2004) Enhancement of hematopoietic stem cell repopulating capacity and self-renewal in the absence of the transcription factor C/EBPα. *Immunity* 21:853–863.
17. Kageyama R, Ohtsuka T, Tomita K (2000) The bHLH gene Hes1 regulates differentiation of multiple cell types. *Mol Cells* 10:1–7.
18. Laiosa C-V, Stadtfeld M, Xie H, de Andres-Aguayo L, Graf T (2006) Reprogramming of committed T cell progenitors to macrophages and dendritic cells by C/EBP alpha and PU.1 transcription factors. *Immunity* 25:731–744.
19. Amsen D, *et al.* (2007) Direct regulation of Gata3 expression determines the T helper differentiation potential of Notch. *Immunity* 27: 89–99.
20. Fang T C, *et al.* (2007) Notch directly regulates Gata3 expression during T helper 2 cell differentiation. *Immunity* 27: 100–110.
21. Tan-Pertel H-T, *et al.* (2000) Notch signaling enhances survival and alters differentiation of 32D myeloblasts. *J Immunol* 165:4428–4436.
22. Ross D-A, Rao P-K, Kadesch T (2004) Dual roles for the Notch target gene Hes-1 in the differentiation of 3T3–L1 preadipocytes. *Mol Cell Biol* 24:3505–3513.
23. Kuhn R, Schwenk F, Aguet M, Rajewsky K (1995) Inducible gene targeting in mice. *Science* 269:1427–1429.
24. Akashi K, Traver D, Miyamoto T, Weissman I-L (2000) A clonogenic common myeloid progenitor that gives rise to all myeloid lineages. *Nature* 404:193–197.
25. Shimizu K, *et al.* (1999) Mouse jagged1 physically interacts with notch2 and other notch receptors: Assessment by quantitative methods. *J Biol Chem* 274:32961–32969.
26. Kitamura T, *et al.* (2003) Retrovirus-mediated gene transfer and expression cloning: Powerful tools in functional genomics. *Exp Hematol* 31:1007–1014.

nature immunology

Notch2 integrates signaling by the transcription factors RBP-J and CREB1 to promote T cell cytotoxicity

Yoichi Maekawa[1,8], Yoshiaki Minato[1,2,8], Chieko Ishifune[1], Takeshi Kurihara[1], Akiko Kitamura[1], Hidefumi Kojima[3], Hideo Yagita[4], Mamiko Sakata-Yanagimoto[5,6], Toshiki Saito[5], Ichiro Taniuchi[7], Shigeru Chiba[5,6], Saburo Sone[2] & Koji Yasutomo[1]

The acquisition of cytotoxic effector function by CD8+ T cells is crucial for the control of intracellular infection and tumor invasion. However, it remains unclear which signaling pathways are required for the differentiation of CD8+ cytotoxic T lymphocytes. We show here that Notch2-deficient T cells had impaired differentiation into cytotoxic T lymphocytes. In addition, dendritic cells with lower expression of the Notch ligand Delta-like 1 induced the differentiation of cytotoxic T lymphocytes less efficiently. We found that the intracellular domain of Notch2 interacted with a phosphorylated form of the transcription factor CREB1, and together these proteins bound the transcriptional coactivator p300 to form a complex on the promoter of the gene encoding granzyme B. Our results suggest that the highly regulated, dynamic control of T cell cytotoxicity depends on the integration of Notch2 and CREB1 signals.

The adaptive immune response is essential for purging a diverse repertoire of invading pathogens and transformed cells[1,2]. $CD8^+$ and $CD4^+$ T cells are required for successful eradication of intracellular pathogens or transformed cells. $CD8^+$ T cells recognize peptides displayed by major histocompatibility complex (MHC) class I molecules (peptide-MHC complexes) on target cells[3]. $CD8^+$ T cells use cytolytic and noncytolytic mechanisms to lyse target cells expressing foreign peptide-MHC complexes. These mechanisms involve perforin and granzymes, as well as cytokines such as interferon-γ (IFN-γ; A001238) and tumor necrosis factor[2–4].

$CD8^+$ T cells responding to specific peptide-MHC complexes undergo considerable changes in gene expression that regulate their differentiation into cytotoxic T lymphocytes (CTLs) and memory cells. Transcriptional regulators activated by T cell receptor (TCR) signaling induce the expression of genes important for directing proliferation, the acquisition of effector functions, and survival. Many transcription factors (such as NF-κB, AP-1 and Jun) expressed in a broad range of cell types are involved in the activation of $CD8^+$ T cells[3]. The T-box transcription factors T-bet and eomesodermin (Eomes) are important inducers of genes involved in the acquisition of $CD8^+$ T cell effector function and in the responsiveness to cytokines that regulate the survival of long-lived memory T cells[5,6]. However, it remains unclear how the transcription of genes encoding cytotoxic effector molecules in CTLs is regulated and how this process influences the direction and differentiation of effector or memory cells.

Notch signaling regulates cell fate 'choice' for a variety of cells[7–9]. Mammals express four Notch receptors and five Notch ligands. The Notch ligands are categorized into two families, Delta and Jagged[8–10], and mice and humans have three genes encoding Delta-like ligands (DL1, DL13 and DL14) and two genes encoding Jagged molecules (Jagged1 and Jagged2). Studies have shown that Notch signaling is involved in early T cell development as well as differentiation into mature $CD4^+$ T cells[7,9,11–19]. However, less is known about the function of Notch in mature $CD8^+$ T cells. One study has shown that constitutive overexpression of DL1 on alloantigen-bearing cells renders these cells nonimmunogenic and able to induce specific nonresponsiveness to a subsequent challenge with the same alloantigen[20]. That study also showed that ligation of Notch on splenic $CD8^+$ cells by purified DL1 protein results in much lower IFN-γ production and concomitantly more production of interleukin 10 (IL-10); these findings suggest that Notch signaling can alter the differentiation potential of $CD8^+$ T cells. However, it did not address whether physiological interaction of Notch with Notch ligands dictates the differentiation of CTLs or memory $CD8^+$ T cells. Furthermore, another report has shown that inhibition of Notch activation results in lower $CD8^+$ T cell proliferation and IFN-γ production[21]. However, that study analyzed Notch function through the use of a γ-secretase

[1]1Department of Immunology & Parasitology and [2]Department of Respiratory Medicine & Rheumatology, Institute of Health Biosciences, The University of Tokushima Graduate School, Tokushima 770-8503, Japan. [3]Department of Immunology, Dokkyo Medical University, Tochigi 321-0293, Japan. [4]Department of Immunology, Juntendo University School of Medicine, Tokyo 113-8421, Japan. [5]5Department of Cell Therapy and Transplantation Medicine, University of Tokyo, Tokyo 113-8655, Japan. [6]Department of Clinical and Experimental Hematology, Graduate School of Comprehensive Human Sciences, University of Tsukuba, Tsukuba 305-8575, Japan. [7]Laboratory for Transcriptional Regulation, RIKEN Research Center for Allergy and Immunology, Yokohama 230-0045, Japan. [8]These authors contributed equally to this work. Correspondence should be addressed to K.Y. (yasutomo@basic.med.tokushima-u.ac.jp).

Received 28 May; accepted 29 July; published online 24 August 2008; doi:10.1038/ni.1649

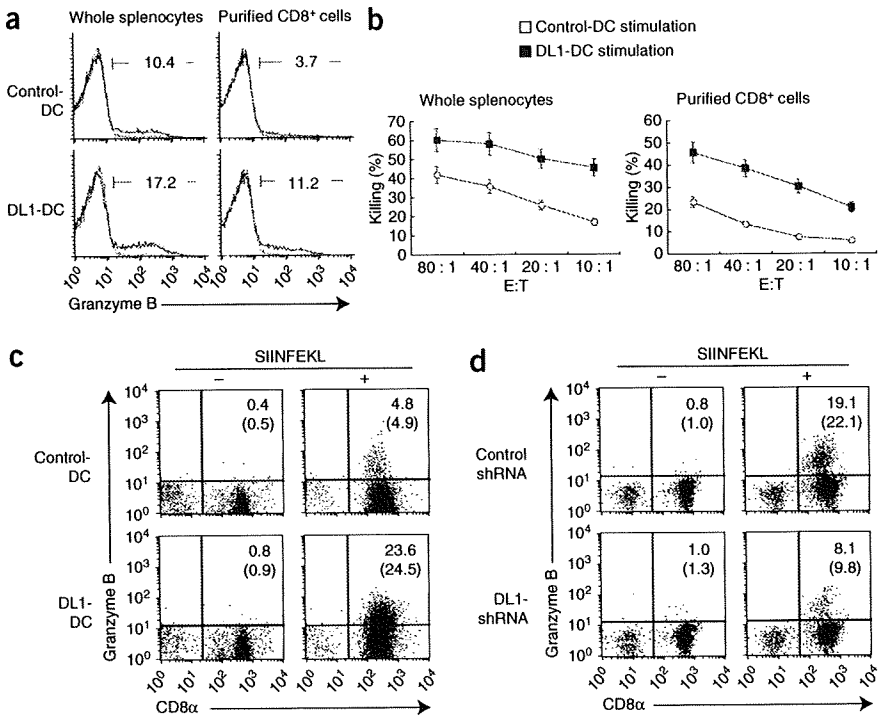

Figure 1 Notch signals control cytotoxic T cell differentiation *in vitro* and *in vivo*. (**a**,**b**) Flow cytometry (**a**) and ^{51}Cr-release assays (**b**) of total spleen T cells (Whole splenocytes) and purified CD8$^+$ cells from BALB/c mice, stimulated with DL1-DCs or control-DCs at a ratio of 10:1. (**a**) or at various ratios (**b**). (**a**) Granzyme B expression in CD8$^+$ T cells 3 d after stimulation. Numbers above bracketed lines indicate percent granzyme B–positive cells. (**b**) Cytolytic activity against EL-4 cells after 5 d of stimulation. E:T, effector/target. Data are representative of five independent experiments (error bars (**b**), s.d.). (**c**,**d**) Flow cytometry of granzyme B expression in splenocytes from B6 mice that received CD8$^+$ T cells from OT-I TCR–transgenic mice, then were inoculated twice with unpulsed (–) or OT-I peptide (SIINFEKL)-pulsed (+) control-DCs or DL1-DCs (**c**) or DCs transduced with DL1-specific shRNA (DL1-shRNA) or control shRNA (**d**), assessed 4 d after the second inoculation of DCs and gated on $V_\alpha2^+V_\beta5^+$ cells. Numbers in plots indicate percent granzyme B–positive cells (top) and percent total $V_\alpha2^+V_\beta5^+$CD8$^+$ cells among splenocytes (below in parentheses). Data are representative of at least four independent experiments.

inhibitor, which may affect other substrates instead of Notch specifically[8]. Therefore, the functions of Notch in CD8$^+$ T cell differentiation remain controversial.

In this report, we show that signaling mediated by Notch2 (A001671) was required for full cytotoxic activity of CTLs and that Notch2 directly controlled transcription of the gene encoding granzyme B (*Gzmb*), which is independent of Eomes. Furthermore, the transcriptional control of *Gzmb* by Notch2 signaling required the molecular interaction of Notch and the transcription factor CREB1 (A000690) in a stable complex on the *Gzmb* promoter. Our results indicate that the Notch and cyclic AMP–responsive element (CRE) pathways intersect to dynamically regulate transcription of CTL effector molecules. In addition, our findings suggest that Notch2 may act as a mechanism directing CD8$^+$ T cell cytolytic function in response to appropriate extrinsic stimuli.

RESULTS

DL1 promotes CTL differentiation

To assess the involvement of Notch signaling in CTL function, we stimulated total spleen cells or purified CD8$^+$ T cells from BALB/c mice with allogeneic bone marrow–derived dendritic cells (BMDCs) obtained from C57BL/6 (B6) mice and infected with a control retrovirus (control-DCs) or the same retrovirus encoding DL1 (DL1-DCs). The control-DCs expressed DL1, and infection with the DL1-encoding retrovirus further increased DL1 expression on the cell surface (**Supplementary Fig. 1a** online). Granzyme B production was much higher in total spleen cells and purified CD8$^+$ T cells after stimulation with DL1-DCs than after stimulation with control-DCs (**Fig. 1a**). Consistent with their higher expression of granzyme B, CD8$^+$ T cells stimulated with DL1-DCs lysed allogeneic EL-4 (mouse thymoma) target cells more efficiently than did CD8$^+$ T cells stimulated with control-DCs (**Fig. 1b**). The granzyme B production in CD8$^+$ T cells and the cytotoxic activity of CD8$^+$ T cells were higher for stimulated total spleen cells than for stimulated purified CD8$^+$ T cells. There was similarly less granzyme B production in splenocyte samples depleted of CD4$^+$ T cells than in total spleen cells (**Supplementary Fig. 1b**). These data suggest CD4$^+$ T cells stimulated by allogeneic spleen cells enhance the generation of CTLs. Published papers have shown that CD4$^+$ T cells are directly or indirectly involved in promoting the generation of CTLs[22,23]. We found that CD4$^+$ T cells cultured with allogeneic DCs promoted upregulation of DL1 expression on these DCs (**Supplementary Fig. 1c**); this observation suggests that CD4$^+$ T cells may be indirectly involved in providing Notch signals to CD8$^+$ T cells. Another possibility is that CD4$^+$ T cells activated by allogeneic DCs directly 'help' CTL differentiation, which is further enhanced by DL1 expressed on DCs. Although further analyses are needed to clarify the mechanism by which CD4$^+$ T cells enhance CTL differentiation in our experimental systems, these data indicate that DL1-mediated signals 'preferentially' direct CTL differentiation *in vitro*.

To test the hypothesis that DL1-mediated signaling contributes to CTL differentiation *in vivo*, we pulsed control-DCs or DL1-DCs with OT-I peptide (SIINFEKL) and injected the cells intravenously twice into B6 mice that had previously received T cells from mice transgenic for an OT-I T cell receptor (TCR), which express a $V_\alpha2V_\beta5$ TCR specific for SIINFEKL presented by H-2K^b. We evaluated the generation of OT-I-specific CTLs by staining the cells with $V_\alpha2$- and $V_\beta5$-specific antibodies 4 d after the second injection of peptide-pulsed DCs. The proportion of granzyme B–producing $V_\alpha2^+V_\beta5^+$CD8$^+$ T cells (called 'OT-I T cells' here) was higher in mice that received DL1-DCs than in those that received control-DCs (**Fig. 1c**), which indicates that DL1 can augment CTL differentiation *in vivo*.

We next investigated whether lower expression of DL1 on DCs impairs the generation of CTLs. We induced BMDCs *in vitro* with granulocyte-macrophage colony-stimulating factor and IL-4, retrovirally transduced the cells with control short hairpin RNA (shRNA) or DL1-specific shRNA, then pulsed them with OT-I peptide. The bicistronic retrovirus vector also encoded green fluorescence protein (GFP), which allowed us to identify infected cells and confirm shRNA-mediated suppression of DL1 surface expression (**Supplementary**

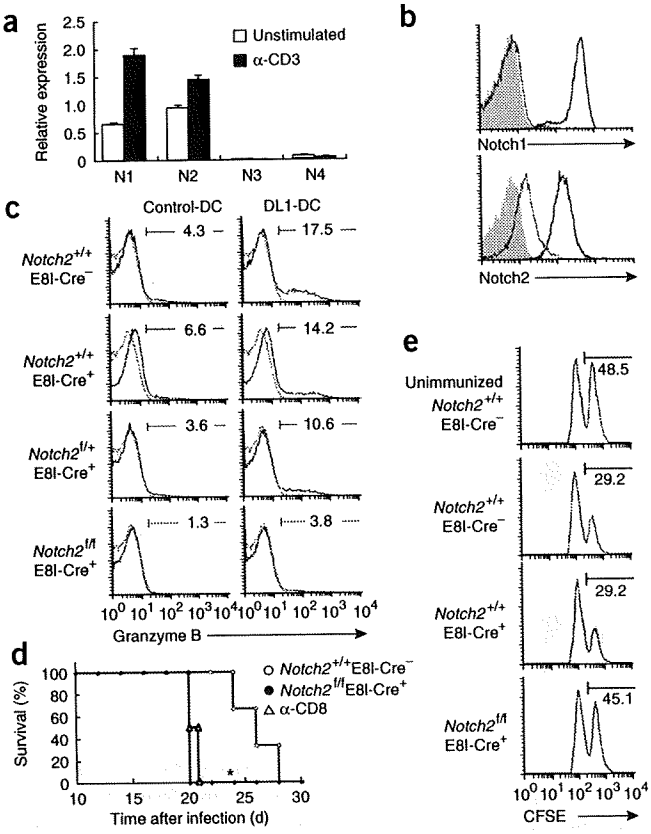

Figure 2 Notch2 on CD8$^+$ T cells promotes CTL induction *in vitro* and *in vivo*. (**a**) Quantitative PCR of the expression of Notch1–Notch4 (N1–N4) in naive CD8$^+$ T cells (Unstimulated) and activated CD8$^+$ T cells stimulated with anti-CD3 (α-CD3), normalized to *Gapdh* mRNA and presented as 'fold increase' relative to *Notch2* expression in naive CD8$^+$ T cells. Data are representative of three independent experiments (mean and s.d. of three samples). (**b**) Flow cytometry of the expression of Notch1 and Notch2 in total spleen cells (CD8$^+$ T cells) left unstimulated (thin lines) or stimulated for 24 h with soluble anti-CD3 (5 μg/ml; thick lines). Shaded histograms, naive CD8$^+$ cells stained with streptavidin-allophycocyanin alone. Data are representative of five independent experiments. (**c**) Flow cytometry of the expression of granzyme B in purified CD8$^+$ cells from *Notch2*$^{+/+}$ E8I-Cre$^-$, *Notch2*$^{+/+}$E8I-Cre$^+$. *Notch2*$^{f/+}$E8I-Cre$^+$ or *Notch2*$^{f/f}$E8I-Cre$^+$ mice, stimulated with BALB/c control-DCs or DL1-DCs, analyzed 3 d after stimulation. Thin lines, isotype-matched control antibody; thick lines, anti–granzyme B. Numbers above bracketed lines indicate percent granzyme B–positive cells among total CD8$^+$ cells. Data are representative of five independent experiments. (**d**) Survival of mice after intraperitoneal infection with *T. cruzi* (2×10^3 trypomastigotes), assessed in *Notch2*$^{+/+}$E8I-Cre$^-$ and *Notch2*$^{f/f}$E8I-Cre$^+$ mice treated with control rat IgG and wild-type mice treated with antibody to mouse CD8β (α-CD8). *, $P = 0.0253$, wild-type versus *Notch2*$^{f/f}$E8I-Cre$^+$ (log-rank test). Data are representative of three independent experiments. (**e**) Flow cytometry of CFSE expression in splenocytes from unimmunized *Notch2*$^{+/+}$E8I-Cre$^-$mice (top) or mice preimmunized with SIINFEKL-pulsed DCs (below), assessed 1 d after injection of a 1:1 mixture of SIINFEKL-pulsed spleen cells labeled with a high concentration of CFSE and unpulsed spleen cells labeled with a low concentration of CFSE. Numbers above bracketed lines indicate percent CFSE^{hi} cells. Data are representative of three independent experiments.

Fig. 1d). We isolated GFP$^+$CD11c$^+$ DCs and injected them intravenously into B6 mice previously injected with OT-1 T cells. Approximately 20% of splenic OT-I T cells expressed granzyme B in mice that received DCs transduced with control shRNA, whereas only 8% did so in mice that received DCs transduced with DL1-specific shRNA (**Fig. 1d**). Furthermore, the absolute number of OT-I T cells in the spleen was also lower in mice that received DCs transduced with DL1-specific shRNA than in mice that received DCs transduced with control shRNA ($5.2 \times 10^5 \pm 1.2 \times 10^5$ cells per spleen versus $9.0 \times 10^5 \pm 1.3 \times 10^5$ cells per spleen, respectively; $n = 5$ mice per experiment; $P < 0.01$). These data collectively demonstrate that DL1 on DCs is required for optimal CTL differentiation *in vivo*, although it is possible that other cells expressing DL1 may contribute to CTL differentiation.

Notch2 controls CTL differentiation

Naive CD8$^+$ T cells expressed Notch1 and Notch2 mRNA, and both transcripts were upregulated after stimulation with antibody to CD3 (anti-CD3; **Fig. 2a**). Naive and activated CD8$^+$ T cells had extremely low expression of Notch3 and Notch4 (**Fig. 2a**). We detected expression of Notch2 but not of Notch1 on the surface of naive CD8$^+$ T cells by flow cytometry (**Fig. 2b**). However, cell surface expression of both Notch1 and Notch2 was also rapidly upregulated after CD3 cross-linking (**Fig. 2b**).

To evaluate the contribution of Notch signaling to CTL differentiation, we crossed mice expressing a *lox*P-flanked (floxed) gene encoding Notch2 (*Notch2*$^{f/f}$) with mice expressing Cre recombinase driven by a combination of the core E8I enhancer and the *Cd8a* promoter (called 'E8I-Cre' here). E8I-Cre was expressed specifically in peripheral CD8$^+$ T cells (data not shown). *Notch2*$^{f/f}$E8I-Cre$^+$ mice lacked Notch2 expression in peripheral CD8$^+$ T cells but not CD4$^+$ T cells (**Supplementary Fig. 2a** online). CD8$^+$ T cells from *Notch2*$^{f/f}$E8I-Cre$^+$ mice had less production of granzyme B than did those from *Notch2*$^{+/+}$E8I-Cre$^-$, *Notch2*$^{+/+}$E8I-Cre$^+$ or *Notch2*$^{f/+}$E8I-Cre$^+$ mice after stimulation with allogeneic control-DCs or DL1-DCs *in vitro* (**Fig. 2c**). CD8$^+$ T cells from *Notch2*$^{f/+}$E8I-Cre$^+$mice also had less production of granzyme B than did those from *Notch2*$^{+/+}$E8I-Cre$^-$ or *Notch2*$^{+/+}$E8I-Cre$^+$ mice, which indicated haploinsufficiency of Notch2 in terms of CTL differentiation.

To evaluate the effect of Notch2 deficiency on CTL induction *in vivo*, we infected *Notch2*$^{+/+}$E8I-Cre$^-$ and *Notch2*$^{f/f}$E8I-Cre$^+$ mice with the intracellular protozoan parasite *Trypanosoma cruzi* (**Fig. 2d**). The acute phase of *T. cruzi* infection is controlled by CTLs expressing granzyme B and perforin[24]. We monitored the survival of *Notch2*$^{+/+}$E8I-Cre$^-$ and *Notch2*$^{f/f}$E8I-Cre$^+$ mice after *T. cruzi* infection and found significantly earlier death of *Notch2*$^{f/f}$E8I-Cre$^+$ mice than of *Notch2*$^{+/+}$E8I-Cre$^-$ mice (**Fig. 2d**). Although the control mice eventually died after this infection, the mortality of *Notch2*$^{f/f}$E8I-Cre$^+$ mice after *T. cruzi* infection was similar to that of wild-type mice depleted of CD8$^+$ T cells (**Fig. 2d**), which indicates that Notch2 is a chief contributor to CD8$^+$ T cell effector function in this experimental system. The expression of Cre itself in CD8$^+$ T cells did not have any influence on the course of *T. cruzi* infection (**Supplementary Fig. 2b**). As the course of *T. cruzi* infection is affected by many factors other than CTLs, we used an *in vivo* CTL assay to further examine the importance of Notch2 in controlling CTL function (**Fig. 2e**). We immunized *Notch2*$^{+/+}$E8I-Cre$^-$, *Notch2*$^{+/+}$E8I-Cre$^+$ or *Notch2*$^{f/f}$E8I-Cre$^+$ mice with OT-I peptide–pulsed DCs, then, 4 d later, gave the mice spleen cells labeled with the cytosolic dye CFSE (carboxyfluorescein diacetate succinimidyl diester) at a high concentration and pulsed with OT-I peptide or gave them spleen cells labeled with CFSE alone at a low concentration. We then compared the ratio of CFSE^{hi} cells to CFSE^{lo} cells at 24 h after cell transfer. *Notch2*$^{+/+}$E8I-Cre$^-$ and *Notch2*$^{+/+}$E8I-Cre$^+$ mice showed 'preferential' killing of peptide-pulsed spleen cells, whereas *Notch2*$^{f/f}$E8I-Cre$^+$ mice showed little killing of either injected population (**Fig. 2e**). These data collectively indicate that Notch2 transduces an important signal for

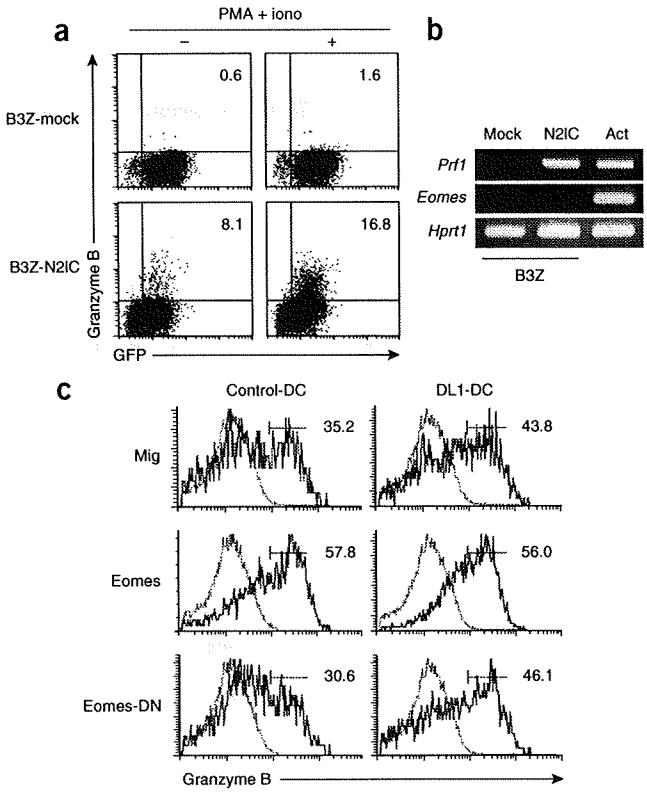

Figure 3 Notch2 signaling induces the transcription of genes encoding CTL effector molecules independently of Eomes. (**a**) Granzyme B expression in B3Z-N2IC and B3Z-mock cells with (+) or without (–) stimulation with PMA and ionomycin (PMA + iono). GFP encoded by the bicistronic retrovirus 'marks' infected cells; numbers in top right quadrants indicate percent granzyme B–positive GFP$^+$ cells. Data are representative of five independent experiments. (**b**) RT-PCR analysis of the expression of Eomes or perforin (*Prf1*) by B2Z-mock cells (Mock) or B3Z-N2IC cells (N2IC) or OT-I-transgenic CD8$^+$ T cells stimulated for 24 h with SIINFEKL peptide (Act). Data are representative of five independent experiments. (**c**) Flow cytometry of granzyme B expression by CD8$^+$GFP$^+$ cells among OT-I-transgenic CD8$^+$ T cells stimulated with SIINFEKL-pulsed DL1-DCs or control-DCs and transduced with vector alone (Mig), Eomes or Eomes-DN. Thin lines, isotype-matched control antibody; Thick lines, anti–granzyme B. Numbers above bracketed lines indicate percent granzyme B–positive cells among total CD8$^+$ cells. Data are representative of four independent experiments.

CTL differentiation *in vitro* and *in vivo*, even if Notch1 is also expressed on CD8$^+$ T cells.

Notch2 promotes the expression of cytotoxic molecules

We next tested if Notch2 signaling directly controls the expression of cytotoxic effector molecules. For this, we transduced the active form of Notch2 (its intracellular domain; N2IC) into a CD8$^+$ T cell–derived hybridoma (B3Z). B3Z cells expressed neither granzyme B nor perforin; however, transduction of N2IC into B3Z cells (B3Z-N2IC cells) induced the expression of both molecules, even in the absence of TCR stimulation (**Fig. 3a,b**). Stimulation of B3Z-N2IC cells with phorbol 12-myristate 13-acetate (PMA) and ionomycin further upregulated granzyme B expression (**Fig. 3a**), whereas this stimulation did not induce granzyme B expression in B3Z cells transduced with control vector (B3Z-mock cells). These results suggest that Notch2 signaling controls the expression of granzyme B mRNA and perforin mRNA.

The T-box transcription factor Eomes controls effector CD8$^+$ T cell function[5]. Although activated CD8$^+$ T cells expressed Eomes, B3Z-N2IC cells did not express Eomes (**Fig. 3b**). As suggested before[5], transduction of Eomes into CD8$^+$ T cells upregulated granzyme B expression, whereas transduction of a dominant negative form of Eomes (Eomes-DN) suppressed granzyme B expression slightly (**Fig. 3c**). However, transduction of Eomes-DN into activated CD8$^+$ T cells from OT-I TCR–transgenic mice did not suppress DL1-mediated upregulation of granzyme B (**Fig. 3c**). Furthermore, overexpression of Eomes in B3Z cells did not induce granzyme B expression, even after stimulation with PMA and ionomycin (**Supplementary Fig. 3a** online). In addition, overexpression of Eomes in B3Z cells upregulated IFN-γ only after stimulation with PMA and ionomycin (**Supplementary Fig. 3a**). The stimulation of CD8$^+$ T cells by DL1-DCs also enhanced IFN-γ expression relative to that induced by control-DCs, but this enhancement was inhibited by transduction with Eomes-DN (**Supplementary Fig. 3b**). These findings collectively demonstrate that Notch2 controls T cell expression of granzyme B independently of Eomes and controls IFN-γ in a way dependent on Eomes.

The proximal region of the *Gzmb* promoter contains several binding elements for the DNA-binding protein RBP-J, which, after binding to the intracellular domain of Notch, is converted from a transcriptional repressor to a transcriptional activator; RBP-J-binding elements are called 'RBEs' (**Supplementary Fig. 4** online). We used a luciferase assay to evaluate whether *Gzmb* promoter activity was influenced by Notch signaling. B3Z-N2IC cells had *Gzmb* promoter activity that was five- to tenfold higher than that of control B3Z-mock cells. Deletion and substitution of RBEs showed that the region containing the most proximal RBE was necessary for N2IC-induced promoter activity (**Fig. 4a,b**). We then confirmed by chromatin immunoprecipitation direct binding of RBP-J to this proximal RBE region in the *Gzmb* promoter in parent B3Z cells (**Fig. 4c**). To confirm direct binding of N2IC to this RBE, we did chromatin immunoprecipitation with anti-Myc in B3Z cells transduced with Myc-tagged N2IC (**Fig. 4d**). We detected the RBE amplicon in the anti-Myc chromatin immunoprecipitates of B3Z cells transduced with Myc-tagged N2IC but not those of B3Z-mock cells. We next determined whether Notch2 controls the transcription of perforin. In a promoter assay using the 2,300–base pair region upstream of the transcription initiation site of the gene encoding perforin, B3Z-N2IC cells had higher activity of the perforin promoter than did control B3Z-mock cells (**Supplementary Fig. 5a** online). We confirmed by chromatin immunoprecipitation that RBP-J directly bound to an RBE 140 base pairs upstream of the transcription initiation site of perforin (**Supplementary Fig. 5b**). These results demonstrate that Notch2 signaling directly regulates transcription of genes encoding the crucial CTL effector molecules granzyme B and perforin.

We found that the region 40 base pairs downstream of the most proximal RBE was also critical for activation of the *Gzmb* promoter in B3Z-N2IC cells (**Fig. 4a**). This region contained a CRE site (**Supplementary Fig. 4**), and mutation of this CRE site also decreased *Gzmb* promoter activity (**Fig. 4e**). The effects of RBE and CRE mutation were similar in magnitude, in terms of *Gzmb* promoter activity, in primary CD8$^+$ T cells from B6 mice stimulated with allogeneic BALB/c BMDCs transduced with DL1 (**Fig. 4f**). These findings indicate that both the RBE and CRE are required for Notch2-mediated expression of granzyme B.

Notch2 interacts with CREB1

We next assessed whether CRE-binding proteins are involved in CTL differentiation. CREB1 activity is regulated by protein kinase A[25]. CREB1 recruits the transcriptional coactivator p300 (A001716) through phosphorylation of the serine residue at position 133 of

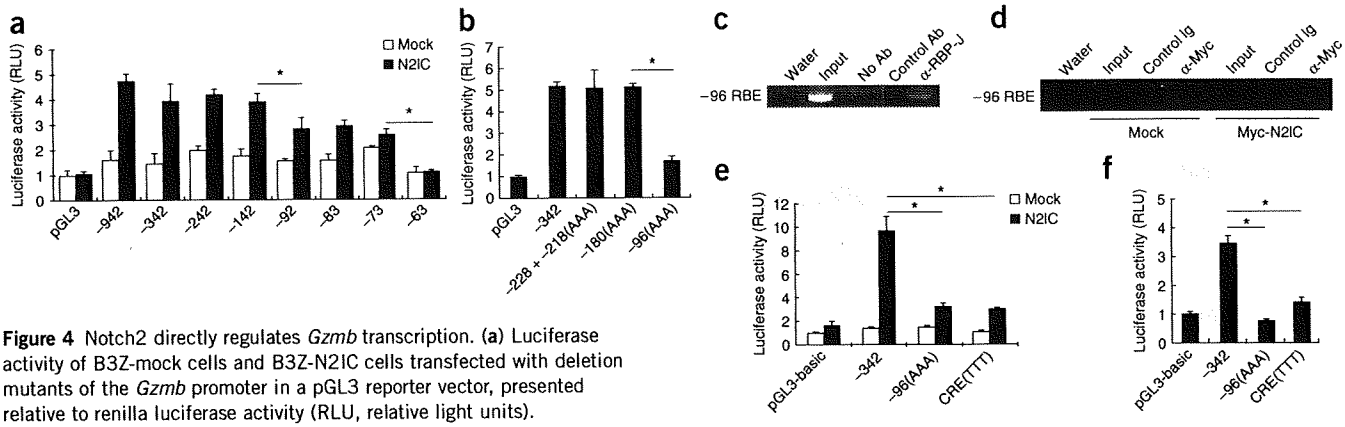

Figure 4 Notch2 directly regulates *Gzmb* transcription. **(a)** Luciferase activity of B3Z-mock cells and B3Z-N2IC cells transfected with deletion mutants of the *Gzmb* promoter in a pGL3 reporter vector, presented relative to renilla luciferase activity (RLU, relative light units). Horizontal axis, position of initial nucleotide of deletion mutant, relative to the transcription start site ('pGL3-basic' indicates vector only). *, $P < 0.05$. **(b)** Luciferase activity of B3Z-mock and B3Z-N2IC cells transfected with pGL3 vector encoding regions of the *Gzmb* promoter with mutations at various RBE sites (**Supplementary Fig. 4**), relative to that of cells transfected with the wild-type *Gzmb* promoter. *, $P < 0.05$. **(c)** Chromatin-immunoprecipitation analysis of fixed and sonicated B3Z cells immunoprecipitated with anti-RBP-J or control antibody (Ab); complexes were treated with protease and the resultant DNA was amplified by primers specific for the *Gzmb* promoter region containing an RBE 96 base pairs upstream of the transcription initiation site (–96 RBE). Water, no template DNA; Input, total DNA before immunoprecipitation. **(d)** Chromatin-immunoprecipitation analysis of B3Z cells transduced with mock or Myc-tagged N2IC vectors, then fixed and lysed; enzymatically sheared chromatin DNA was immunoprecipitated with anti-Myc or control mouse IgG, followed by DNA amplification as described in **c**. **(e)** Luciferase activity of B3Z-mock and B3Z-N2IC cells transfected with pGL3 plasmid vectors containing mutated *Gzmb* promoters (**Supplementary Fig. 4**), presented relative to renilla luciferase activity. CRE(TTT), CRE with three thymine substitutions. *, $P < 0.05$. **(f)** Luciferase activity of $CD8^+$ T cells first purified from BALB/c splenocytes stimulated for 3 d with B6 BMDCs, then, after purification, transfected with *Gzmb* promoter–driven luciferase constructs (**Supplementary Fig. 4**) and cultured for 1 d more, presented relative to the activity of cells transfected with pGL3 vector only. *, $P < 0.05$. Data are representative of five (**a–e**) or four (**f**) independent experiments (error bars, s.d., **a,b,e,f**).

CREB1 by cAMP-activated protein kinase A[25]. Transduction of a dominant negative form of CREB1 (A-CREB1), which contains a substitution of alanine for the serine residue at position 133 and is thus incapable of recruiting p300, impaired granzyme B expression in both B3Z-N2IC cells and primary OT-I $CD8^+$ T cells (**Fig. 5a,b**). The effect of A-CREB1 was less apparent in OT-I T cells; this blunted effect might be attributed to the delayed overexpression of A-CREB1, as retrovirus-mediated transduction of A-CREB1 in T cells required preactivation of T cells. Nevertheless, these data demonstrate that Notch2-mediated CTL differentiation requires a CREB1-mediated signal.

To examine the molecular mechanism whereby Notch2 and CREB1 signaling integrate during CTL differentiation, we determined if N2IC interacted with CREB1. When we transfected both CREB1 and Myc-tagged N2IC into human embryonic kidney 293T cells, CREB1 immunoprecipitated together with anti-Myc immunoprecipitates (**Fig. 5c**). In contrast, A-CREB1 did not interact with N2IC (**Fig. 5d**), which indicates that phosphorylation of CREB1 is required for the formation of a complex of CREB1 and N2IC.

Next we used gel-shift assays to examine binding of the N2IC-CREB1 complex to the *Gzmb* promoter. We found a dominant complex with a probe containing wild-type RBE and CRE sites, based on the sequence of the proximal *Gzmb* promoter (**Fig. 6a**). We also detected a faint band on the probe containing wild-type RBE and CRE sites as well as on a probe of wild-type RBE and mutant CRE, but not on a probe of mutant RBE and wild-type CRE (**Fig. 6a**). The mobility of this faint band shifted after the addition of anti-RBP-J, even in B3Z cells (data not shown), which indicated that this band

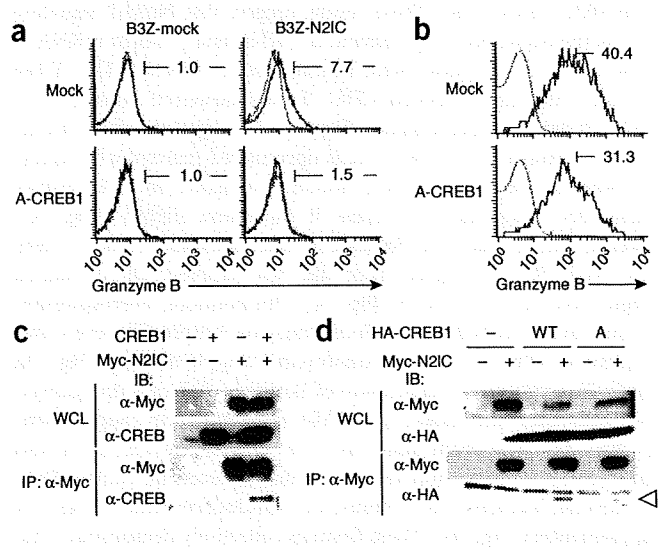

Figure 5 CREB1 is required for Notch2-mediated granzyme B expression through interaction of the intracellular domain of Notch2 with pCREB1. **(a)** Flow cytometry of granzyme B expression by B3Z-N2IC or B3Z-mock cells mock-transfected (top row) or transfected with A-CREB1 in a bicistronic retroviral vector encoding human NGFR, assessed in cells gated as GFP^+ (N2IC) and/or positive for human NGFR (A-CREB1). Thin lines, thick lines, anti–granzyme B. Data are representative of five independent experiments. **(b)** Flow cytometry of granzyme B expression by GFP^+CD8^+ gated cells among OT-I-transgenic T cells stimulated with SIINFEKL peptide and transduced by retroviral vectors encoding GFP with or without A-CREB1. Thin lines, isotype-matched control antibody; thick lines, anti–granzyme B. Data are representative of five independent experiments. **(c)** Immunoblot analysis of N2IC and CREB1 in 293T cells transfected with Myc-tagged N2IC and/or CREB1, detected with anti-Myc and anti-CREB in whole-cell lysates (WCL) and after immunoprecipitation with anti-Myc (IP: α-Myc). Data are representative of five independent experiments. **(d)** Immunoblot analysis of CREB1 and N2IC in 293T cells transfected with hemagglutinin-tagged wild-type CREB1 (WT) or mutant CREB1 (A) with or without Myc-tagged N2IC, detected with anti-Myc and anti-hemagglutinin (α-HA) in whole-cell lysates and after immunoprecipitation with anti-Myc. Arrowhead indicates hemagglutinin-tagged CREB1. Data are representative of three independent experiments.

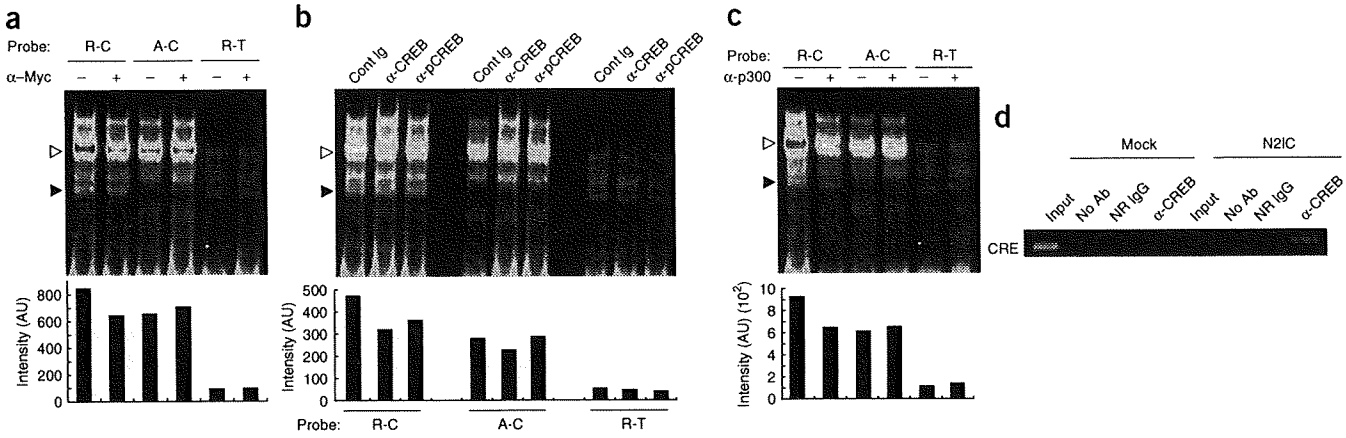

Figure 6 Notch2 interacts with pCREB1 and stably recruits p300 to the *Gzmb* promoter. (**a–c**) Gel-shift assay of nuclear extracts of B3Z-N2IC cells incubated with various probes (top (**a**,**c**) or bottom (**b**)) in the presence or absence of various antibodies (above lanes). R-C, wild-type RBE and wild-type CRE; A-C, mutant RBE and wild-type CRE; R-T, wild-type RBE and mutant CRE. Open arrowheads, dominant CRE-dependent complex; filled arrowheads, RBE-dependent complex. Below, intensity of bands indicated by open arrowheads, presented as arbitrary units (AU). Cont, control. Data are representative of five independent experiments. (**d**) Chromatin-immunoprecipitation analysis of fixed and sonicated B3Z-mock or B3Z-N2IC cells immunoprecipitated with anti-CREB or control antibody; complexes were treated with protease and the resultant DNA was amplified by primers specific for the *Gzmb* promoter region containing a CRE. NR IgG, control isotype antibody. Data are representative of five independent experiments.

corresponded to RBP-J. To determine the composition of the dominant complex, we analyzed the mobility shift or intensity of the band by adding specific antibodies and mutant probes to the nuclear extracts. The addition of antibody to Myc-tagged N2IC decreased the intensity of the dominant complex on the probe containing wild-type RBE and CRE sites to the intensity of the probe of mutant RBE and wild-type CRE (**Fig. 6a**), which indicated that N2IC was one of the components of this complex. Furthermore, the intensity of the dominant band binding to the probe of wild-type RBE and mutant CRE was apparently lower, even if RBP-J bound to this probe (**Fig. 6a**), which indicated that CRE was essential for binding of the dominant complex to DNA. The addition of anti-CREB1 or antibody to CREB1 phosphorylated at the serine residue at position 133 (pCREB1) decreased the intensity of the binding of the dominant complex to that of the probe containing wild-type RBE and CRE sites and, to a lesser extent, to that of the probe of mutant RBE and wild-type CRE (**Fig. 6b**). These findings indicate a requirement for Notch2 signaling for optimal binding of pCREB1 to the probe containing wild-type RBE and CRE sites and also show that pCREB1 is also a component of this dominant complex. The addition of anti-p300 attenuated binding of the dominant complex only to the probe containing wild-type RBE and CRE sites (**Fig. 6c**), which demonstrated that p300 is a component of the dominant complex recruited to the *Gzmb* promoter only when both RBP-J or N2IC and pCREB1 bind simultaneously. As the addition of anti-Notch2 or anti-p300 did not change the intensity of the dominant band on the probe of mutant RBE and wild-type CRE, CRE-binding factors including CREB1 might form a complex without N2IC and p300, and this complex might bind to the probe of mutant RBE and wild-type CRE and migrate to a location similar to that of the dominant complex in the native polyacrylamide gel. These results collectively suggest that the dominant complex identified by the probe containing wild-type RBE and CRE sites is composed of N2IC, pCREB1 and p300. Finally, we tested by chromatin-immunoprecipitation assay whether CREB1 bound directly to the *Gzmb* promoter. We detected binding of CREB1 to the CRE in the *Gzmb* promoter in B3Z-N2IC cells but not in B3Z-mock cells (**Fig. 6d**), which indicates that Notch signaling induces CREB1 to binding to this promoter region.

We propose a model in which in the absence of Notch signaling, RBP-J, together with corepressors, binds to RBEs and suppresses granzyme B transcription (**Supplementary Fig. 6** online). In the presence of Notch2 signaling, both RBEs and CREs are required for stable binding of N2IC, pCREB1 and p300 to the *Gzmb* promoter region; in fact, these three molecules formed a complex on the promoter (**Supplementary Fig. 5**). Single p300 molecules can form a complex with N2IC and pCREB1, as p300 is able to interact with Notch or pCREB1 at distinct domains[26,27]. Moreover, p300 may stabilize the DNA binding of the RBP-J-N2IC-pCREB1 complex and/or strengthen granzyme B transcription. The absence of an RBE probably allows unphosphorylated CREB1 or other CRE-binding factors to bind, which may induce a small amount of *Gzmb* promoter activity, but the presence of RBE and Notch2 signals probably results in exchange of the binding protein from CREB1 to pCREB1, perhaps because a pCREB1-containing complex is more stable on the promoter.

DISCUSSION

The $CD8^+$ T cell response to infection and transformed cells requires the recognition of antigen, massive proliferation and differentiation into CTLs[1]. However, the transcriptional programs that control the differentiation of CTLs during the immune response have not been fully identified. In this report, we have shown that DL1-induced Notch2 signals activated the transcription of granzyme B independently of Eomes. We have also identified previously unknown signaling crosstalk in which Notch2 formed a complex with pCREB1 and p300 on the *Gzmb* promoter; this complex was essential for optimal granzyme B transcription. Our results indicate that Notch signaling is required for the dynamic integration of transcription of genes encoding CTL effector molecules and suggest that Notch2 might allow 'tailoring' of CTL differentiation to appropriate environmental stimuli.

Accumulating data have now provided considerable evidence that the differentiation of mature $CD4^+$ T cells is controlled by Notch signaling[12,14,16,18,28,29]. One study has addressed the functions of Notch signaling in $CD8^+$ T cells by hyperactivating Notch with DL1 (ref. 20). That study found that the ligation of Notch on splenic $CD8^+$ T cells by purified DL1 protein results in less IFN-γ, which suggests an

inhibitory function for Notch signaling in CD8$^+$ T cell activation. However, that study did not address whether that inhibitory effect of DL1 is recapitulated by direct interaction of DL1 and Notch on CD8$^+$ T cells *in vivo*. Furthermore, purified DL1 protein might not be able to completely mimic the effect of membrane-bound DL1. Here we have presented *in vitro* and *in vivo* evidence indicating that downregulation of DL1 on DCs or Notch2 deficiency on CD8$^+$ T cells resulted in much lower expression of molecular effectors necessary for effective CTL function. Our data have provided definitive evidence that Notch2-mediated signaling is important in promoting CTL function. Naive CD8$^+$ T cells express Notch2, which is rapidly upregulated after TCR-mediated signaling. The expression of DL1 and DL4 in DCs is also upregulated by Toll-like receptor signaling[14]. Our data suggest that such upregulation of Notch and Notch ligands by environmental stimuli would be an important step in the promotion of CTL activity in situations necessitating the eradiation of intracellular pathogens. In addition, we have shown that activated CD8$^+$ T cells had high expression of Notch1, but not of Notch3 and Notch4, which suggests a possible contribution of Notch1 to CTL differentiation.

Eomes is a T-box transcription factor that is highly homologous to T-bet and is expressed in activated CD8$^+$ T cells and activated natural killer cells[5,6,30]. Overexpression and antagonism studies with dominant negative proteins suggest that Eomes and T-bet might have cooperative or redundant functions in regulating the genes encoding IFN-γ and cytolytic molecules in CD8$^+$ T cells[5]. However, those studies did not show that Eomes or T-bet directly regulates the transcription of granzyme B or perforin by reporter assays, although they demonstrated by chromatin immunoprecipitation assay that Eomes does bind to *Gzmb* promoter regions[6]. We have shown here that Notch2-mediated signaling directly activated the transcription of genes encoding granzyme B and perforin even in the absence of Eomes expression in B3Z cells and in the presence of a dominant negative form of Eomes in mature T cells. Our data indicate that Notch2 signaling is able to 'prime' the transcription of genes encoding cytotoxic molecules in the absence of Eomes. However, the Notch2-induced higher IFN-γ expression in CTLs was inhibited by a dominant negative form of Eomes. These data suggest that Notch and Eomes have both distinct and overlapping functions in exerting full effector functions of CD8$^+$ T cells.

The precise regulatory mechanisms for the ontogeny, function and survival of effector and memory CD8$^+$ T cells, as well as their lineage relationship, remain controversial[2]. Although we have shown that Notch-mediated signaling directly controlled CTL effector functions, we do not yet know whether Notch signaling is involved in aspects of the memory cell differentiation program. Future efforts should be aimed at determining whether Notch signaling skews naive CD8$^+$ T cells toward CTLs instead of memory CD8$^+$ T cells or contributes to the differentiation of both cell types.

Several papers have suggested there is crosstalk of Notch signaling with other signaling pathways, including those induced by stimulation with bone morphogenetic protein or transforming growth factor-β. Notch interacts with the intracellular bone morphogenetic protein mediator SMAD1 and the transforming growth factor-β mediator SMAD3. SMAD1 interacts with the Notch intracellular domain to activate transcription of the genes encoding the Hes and Hey basic helix-loop-helix factors[31–33]. Whether DNA binding by SMAD1 is essential for synergy with Notch is controversial[32,34]. Notch signaling also acts together with the transcription factor HIF-1α to mediate cellular responses to hypoxia[35]. Our data have provided evidence of a mechanism of crosstalk between the Notch and CREB1 signaling pathways. Notch2 formed a complex with pCREB1 and p300 on the *Gzmb* promoter. The cooperative nature of this complex was shown by the finding that Notch2 and pCREB1 were able to stably bind to the *Gzmb* promoter only when both proteins were present, and both the RBP-J-binding region and CRE were required for full *Gzmb* transcription. Furthermore, blocking the phosphorylation of CREB1 resulted in lower expression of granzyme B, which indicates the biological importance of CREB1 in CTL differentiation.

CRE- and RBP-J-binding elements are widely distributed in the promoter or enhancer regions of many genes. Therefore, it is possible that the interactions noted in the *Gzmb* promoter region occur in other promoter or enhancer regions and thereby amplify and broaden the repertoire of genes influenced by each pathway. For example, because CREB-responsive elements regulate several cytokines, including IL-2 (ref. 36), that are required for CTL population expansion, the interaction between Notch and CREB-responsive genes might be involved in aspects of CTL function other than cytotoxicity. In addition, Notch signaling is crucial for a variety of cell proliferation, tumorigenesis or cell fate 'decisions'[7,28,37,38], and such events may also require cooperation with the CREB pathway[39,40]. Given the diverse functions of Notch in vertebrate and invertebrate embryogenesis, our data provide a basis for investigating a general function for CREB in Notch-directed cellular programs. Our findings may also advocate the manipulation of CREB pathway components as a means of modulating or redirecting Notch-mediated cellular processes. Finally, our results indicate that the manipulation of Notch signaling might have a considerable effect in clinical settings in which more CTL function is desirable (such as in tumor immunotherapy) or less CTL function is desirable (such as in autoimmune diseases).

METHODS

Mice and cell culture. Female B6 and BALB/c mice 6–8 weeks of age were from Japan SLC. *Notch2*$^{f/f}$ mice have been described[41]. For the generation of E8I-Cre-transgenic mice, the 1.6-kilobase core of E8I enhancer fragment was inserted in front of the *Cd8a* promoter, and cDNA encoding Cre and an internal ribosomal entry site–GFP–poly(A) cassette were inserted after the *Cd8a* promoter to generate the E8I-Cre transgene (I.T., data not shown). The transgene was expressed in CD8α$^+$CD8β$^+$ αβT cells and CD8αα$^+$CD8β$^-$ αβ T cells but not in CD4$^+$CD8α$^-$CD8β$^-$ αβT cells (data not shown). OT-I TCR–transgenic mice were from Immuno-Biological Laboratories. All animal work was approved by the Animal Research Committee of The University of Tokushima. DCs were generated from mouse bone marrow. Bone marrow cells were treated with anti-CD4 (GK1.5; 14-0041), anti-CD8 (53-6.7; 14-0081), anti-B220 (RA3-6B2; 14-0452) and anti-CD11b (M1/70; 14-0112; all from eBiosciences), followed by magnetic depletion of labeled cells with anti–rat immunoglobulin G (IgG) Dynabeads (Invitrogen). Isolated cells were cultured for 7 d in the presence of granulocyte-macrophage colony-stimulating factor and IL-4. In some experiments, bone marrow cells were infected three times (days 0, 1 and 2) with retrovirus. At 5 d after the final retrovirus infection, cells were stimulated overnight with anti-CD40 (5 μg/ml; 3/23; 553787; BD Biosciences) and LPS (5 μg/ml). After the stimulation, samples were enriched for CD11c$^+$ cells by magnetic separation with CD11c microbeads (MACS; Miltenyi Biotec). In some experiments, GFP$^+$ and CD11c$^+$ cells were purified with a cell sorter (JSAN; Bay Bioscience). The DCEK fibroblast cell line was infected with the DL1-pKE004–human nerve growth factor receptor (NGFR) bicistronic retrovirus. Cells expressing human NGFR were identified by staining with biotin-conjugated antibody to human NGFR and were enriched with streptavidin-conjugated MACS beads. DL1-transduced DCEK cells were further infected with retrovirus containing DL1-specific shRNA or control shRNA in the vector pFB-SIN. B3Z cells were infected with retrovirus encoding N2IC, Eomes or Eomes-DN and were cultured in RPMI 1640 medium supplemented with 10% (vol/vol) FCS. For depletion of CD4$^+$ T cells, splenocytes were labeled with anti-CD4, followed by magnetic depletion of labeled cells with anti–rat IgG Dynabeads (Invitrogen). Samples were enriched for CD8$^+$ cells by magnetic separation with CD8 microbeads (MACS; Miltenyi Biotec). For transduction of

genes into OT-I T cells, retroviruses were added 1 d after stimulation. Cells were fixed with paraformaldehyde and were stained with anti–granzyme B or anti-IFN-γ in buffer containing saponin. After washing, expression of granzyme B or IFN-γ was evaluated by flow cytometry.

PCR. Total RNA was extracted with TRIzol (Invitrogen). After reverse transcription with the Omniscript RT Kit (Qiagen), SYBR *Premix Ex Taq* II (Takara Bio) and primer sets (**Supplementary Table 1** online) were used for quantitative PCR. All data are normalized to *Gapdh* mRNA (encoding glyceraldehyde phosphate dehydrogenase) and are presented as 'fold increase' relative to Notch2 expression in naive $CD8^+$ T cells. Pyrobest polymerase (Takara) and primer sets (**Supplementary Table 1**) were used for conventional PCR.

Statistical methods. The distributed data from interval scales were analyzed with Student's *t*-test; a *P* value of less than 0.05 was considered statistically significant. JMP7 software (SAS institute) was used for the log-rank test.

Additional methods. Information on antibodies, vectors, retrovirus preparation, CTL induction *in vitro* and *in vivo*, *T. cruzi* infection, luciferase assay, immunoprecipitation, chromatin immunoprecipitation and gel-shift assay is available in the **Supplementary Methods** online.

Accession codes. UCSD-Nature Signaling Gateway (http://www.signaling-gateway.org): A001238, A001671, A000690 and A001716.

Note: Supplementary information is available on the Nature Immunology website.

ACKNOWLEDGMENTS

We thank T. Kitamura (Tokyo University), S. Reiner (University of Pennsylvania) and J. Fujisawa (Kansai Medical University) for reagents; R. Germain (US National Institutes of Health) for the DCEK cell line and for discussions; K. Ikuta for critical review of the manuscript; C. Kinouchi for technical assistance; and K. Yamakawa for secretarial assistance. Supported by the Japan Society for the Promotion of Science (Grant-in-Aid for Young Scientists (S)), The Ministry of Education, Culture, Sports, Science and Technology (Grant-in-Aid for Scientific Research on Priority Areas), the Takeda Science Foundation, the Sumitomo Foundation and the Mochida Memorial Foundation.

AUTHOR CONTRIBUTIONS

Y.Ma., Y.Mi., C.I., T.K., A.K. and H.K. did research and analyzed data; H.Y. established antibodies; M.S.-Y., T.S., I.T., and S.C. established genes modified mice; S.S. provided advice for the experiments; and Y.Ma. and K.Y. designed research and wrote the paper.

Published online at http://www.nature.com/natureimmunology/
Reprints and permissions information is available online at http://npg.nature.com/reprintsandpermissions/

1. Wong, P. & Pamer, E.G. CD8 T cell responses to infectious pathogens. *Annu. Rev. Immunol.* **21**, 29–70 (2003).
2. Williams, M.A. & Bevan, M.J. Effector and memory CTL differentiation. *Annu. Rev. Immunol.* **25**, 171–192 (2007).
3. Glimcher, L.H., Townsend, M.J., Sullivan, B.M. & Lord, G.M. Recent developments in the transcriptional regulation of cytolytic effector cells. *Nat. Rev. Immunol.* **4**, 900–911 (2004).
4. Antia, R., Ganusov, V.V. & Ahmed, R. The role of models in understanding $CD8^+$ T-cell memory. *Nat. Rev. Immunol.* **5**, 101–111 (2005).
5. Pearce, E.L. *et al.* Control of effector $CD8^+$ T cell function by the transcription factor Eomesodermin. *Science* **302**, 1041–1043 (2003).
6. Intlekofer, A.M. *et al.* Effector and memory $CD8^+$ T cell fate coupled by T-bet and eomesodermin. *Nat. Immunol.* **6**, 1236–1244 (2005).
7. Radtke, F., Wilson, A., Mancini, S.J. & MacDonald, H.R. Notch regulation of lymphocyte development and function. *Nat. Immunol.* **5**, 247–253 (2004).
8. Maillard, I., Fang, T. & Pear, W.S. Regulation of lymphoid development, differentiation, and function by the Notch pathway. *Annu. Rev. Immunol.* **23**, 945–974 (2005).
9. Osborne, B.A. & Minter, L.M. Notch signalling during peripheral T-cell activation and differentiation. *Nat. Rev. Immunol.* **7**, 64–75 (2007).
10. Louvi, A. & Artavanis-Tsakonas, S. Notch signalling in vertebrate neural development. *Nat. Rev. Neurosci.* **7**, 93–102 (2006).
11. Pear, W.S. & Radtke, F. Notch signaling in lymphopoiesis. *Semin. Immunol.* **15**, 69–79 (2003).
12. Maekawa, Y. *et al.* Delta1-Notch3 interactions bias the functional differentiation of activated $CD4^+$ T cells. *Immunity* **19**, 549–559 (2003).
13. Tsukumo, S. & Yasutomo, K. Notch governing mature T cell differentiation. *J. Immunol.* **173**, 7109–7113 (2004).
14. Amsen, D. *et al.* Instruction of distinct CD4 T helper cell fates by different notch ligands on antigen-presenting cells. *Cell* **117**, 515–526 (2004).
15. Zuniga-Pflucker, J.C. T-cell development made simple. *Nat. Rev. Immunol.* **4**, 67–72 (2004).
16. Tanaka, S. *et al.* The interleukin-4 enhancer CNS-2 is regulated by Notch signals and controls initial expression in NKT cells and memory-type CD4 T cells. *Immunity* **24**, 689–701 (2006).
17. Tanigaki, K. *et al.* Regulation of αβ/γδ T cell lineage commitment and peripheral T cell responses by Notch/RBP-J signaling. *Immunity* **20**, 611–622 (2004).
18. Amsen, D. *et al.* Direct regulation of Gata3 expression determines the T helper differentiation potential of Notch. *Immunity* **27**, 89–99 (2007).
19. Fang, T.C. *et al.* Notch directly regulates Gata3 expression during T helper 2 cell differentiation. *Immunity* **27**, 100–110 (2007).
20. Wong, K.K. *et al.* Notch ligation by Delta1 inhibits peripheral immune responses to transplantation antigens by a $CD8^+$ cell-dependent mechanism. *J. Clin. Invest.* **112**, 1741–1750 (2003).
21. Palaga, T., Miele, L., Golde, T.E. & Osborne, B.A. TCR-mediated Notch signaling regulates proliferation and IFN-γ production in peripheral T cells. *J. Immunol.* **171**, 3019–3024 (2003).
22. Clarke, S.R. The critical role of CD40/CD40L in the CD4-dependent generation of $CD8^+$ T cell immunity. *J. Leukoc. Biol.* **67**, 607–614 (2000).
23. Sallusto, F., Geginat, J. & Lanzavecchia, A. Central memory and effector memory T cell subsets: function, generation, and maintenance. *Annu. Rev. Immunol.* **22**, 745–763 (2004).
24. Muller, U. *et al.* Concerted action of perforin and granzymes is critical for the elimination of *Trypanosoma cruzi* from mouse tissues, but prevention of early host death is in addition dependent on the FasL/Fas pathway. *Eur. J. Immunol.* **33**, 70–78 (2003).
25. Shaywitz, A.J. & Greenberg, M.E. CREB: a stimulus-induced transcription factor activated by a diverse array of extracellular signals. *Annu. Rev. Biochem.* **68**, 821–861 (1999).
26. Oswald, F. *et al.* p300 acts as a transcriptional coactivator for mammalian Notch-1. *Mol. Cell. Biol.* **21**, 7761–7774 (2001).
27. Xu, W., Kasper, L.H., Lerach, S., Jeevan, T. & Brindle, P.K. Individual CREB-target genes dictate usage of distinct cAMP-responsive coactivation mechanisms. *EMBO J.* **26**, 2890–2903 (2007).
28. Bray, S.J. Notch signalling: a simple pathway becomes complex. *Nat. Rev. Mol. Cell Biol.* **7**, 678–689 (2006).
29. Minter, L.M. *et al.* Inhibitors of γ-secretase block *in vivo* and *in vitro* T helper type 1 polarization by preventing Notch upregulation of Tbx21. *Nat. Immunol.* **6**, 680–688 (2005).
30. Intlekofer, A.M., John Wherry, E. & Reiner, S.L. Not-so-great expectations: re-assessing the essence of T-cell memory. *Immunol. Rev.* **211**, 203–213 (2006).
31. Blokzijl, A. *et al.* Cross-talk between the Notch and TGF-β signaling pathways mediated by interaction of the Notch intracellular domain with Smad3. *J. Cell Biol.* **163**, 723–728 (2003).
32. Dahlqvist, C. *et al.* Functional Notch signaling is required for BMP4-induced inhibition of myogenic differentiation. *Development* **130**, 6089–6099 (2003).
33. Takizawa, T., Ochiai, W., Nakashima, K. & Taga, T. Enhanced gene activation by Notch and BMP signaling cross-talk. *Nucleic Acids Res.* **31**, 5723–5731 (2003).
34. Itoh, F. *et al.* Synergy and antagonism between Notch and BMP receptor signaling pathways in endothelial cells. *EMBO J.* **23**, 541–551 (2004).
35. Gustafsson, M.V. *et al.* Hypoxia requires notch signaling to maintain the undifferentiated cell state. *Dev. Cell* **9**, 617–628 (2005).
36. Barton, K. *et al.* Defective thymocyte proliferation and IL-2 production in transgenic mice expressing a dominant-negative form of CREB. *Nature* **379**, 81–85 (1996).
37. Roy, M., Pear, W.S. & Aster, J.C. The multifaceted role of Notch in cancer. *Curr. Opin. Genet. Dev.* **17**, 52–59 (2007).
38. Hurlbut, G.D., Kankel, M.W., Lake, R.J. & Artavanis-Tsakonas, S. Crossing paths with Notch in the hyper-network. *Curr. Opin. Cell Biol.* **19**, 166–175 (2007).
39. Siu, Y.T. & Jin, D.Y. CREB–a real culprit in oncogenesis. *FEBS J.* **274**, 3224–3232 (2007).
40. Chen, A.E., Ginty, D.D. & Fan, C.M. Protein kinase A signalling via CREB controls myogenesis induced by Wnt proteins. *Nature* **433**, 317–322 (2005).
41. Saito, T. *et al.* Notch2 is preferentially expressed in mature B cells and indispensable for marginal zone B lineage development. *Immunity* **18**, 675–685 (2003).

bjh research paper

High incidence of haemophagocytic syndrome following umbilical cord blood transplantation for adults

Shinsuke Takagi,[1] Kazuhiro Masuoka,[1] Naoyuki Uchida,[1] Kazuya Ishiwata,[1] Hideki Araoka,[2] Masanori Tsuji,[1] Hisashi Yamamoto,[1] Daisuke Kato,[1] Yoshiko Matsuhashi,[1] Eiji Kusumi,[1] Yasunori Ota,[3] Sachiko Seo,[1] Tomoko Matsumura,[1] Naofumi Matsuno,[1] Atsushi Wake,[1] Shigesaburo Miyakoshi,[4] Shigeyoshi Makino,[5] Kenichi Ohashi,[3] Akiko Yoneyama[2] and Shuichi Taniguchi[1]

[1]Department of Haematology, Toranomon Hospital, [2]Department of Infectious Diseases, Toranomon Hospital, [3]Department of Pathology, Toranomon Hospital, [4]Department of Haematology, Tokyo Metropolitan Geriatric Hospital, and [5]Department of Transfusion Medicine, Toranomon Hospital, Tokyo, Japan

Received 28 June 2009; accepted for publication 22 July 2009

Correspondence: Naoyuki Uchida, MD, Department of Haematology, Toranomon Hospital, 2-2-2 Toranomon, Minato-Ku, Tokyo 105-0001, Japan.
E-mail: nuchida@toranomon.gr.jp

Statement of prior presentations: Presented in abstract form at the 33th annual congress of the European Group for Blood and Marrow Transplantation, Lyon, France, March 28, 2007.

Summary

Umbilical cord blood transplantation (CBT) is widely accepted, but one critical issue for adult patients is a low engraftment rate, of which one cause is haemophagocytic syndrome (HPS). We aimed to identify the contribution of HPS to engraftment failure after CBT, following preparative regimens containing fludarabine phosphate, in 119 patients (median age, 55 years; range; 17–69 years) with haematological diseases. Graft-*versus*-host disease prophylaxis comprised continuous infusion of a calcineurin inhibitor with or without mycophenolate mofetil. Of the 119 patients, 20 developed HPS within a median of 15 d (cumulative incidence; 16·8%) and 17 of them did so before engraftment. Donor-dominant chimaerism was confirmed in 16 of 18 evaluable patients with HPS. Despite aggressive interventions including corticosteroid, ciclosporin, high-dose immunoglobulin and/or etoposide, engraftment failed in 14 of 18 patients. Of these 14 patients, four received second rescue transplantation and all resulted in successful engraftment. Overall survival rates significantly differed between patients with and without HPS (15·0% vs. 35·4%; $P < 0·01$). Univariate and multivariate analysis identified having fewer infused $CD34^+$ cells as a significant risk factor for the development of HPS ($P = 0·01$ and 0·006, respectively). We concluded that engraftment failure closely correlated with HPS in our cohort, which negatively impacted overall survival after CBT.

Keywords: cord blood transplantation, reduced-intensity chemotherapy, haemophagocytic syndrome, engraftment failure.

Umbilical cord blood transplantation (CBT) is an alternative allogeneic haematopoietic stem cell transplantation (HSCT) strategy for patients with haematological diseases who do not have a matched related or unrelated donor and who need urgent transplantation. The value of CBT using myeloablative preparative regimens has already been confirmed among paediatric and adult patients (Laughlin *et al*, 2004; Rocha *et al*, 2004; Takahashi *et al*, 2004). However, conventional myeloablative preparative regimens are associated with significant morbidity and mortality, particularly in older patients or in those who have experienced extensive prior therapy or organ dysfunction associated with transplantation-related mortality. Various reduced-intensity preparative regimens that have been applied to such patients by several groups, including the authors of the present study, have proven feasible (Barker *et al*, 2003, 2005; Chao *et al*, 2004; Jacobsohn *et al*, 2004; Miyakoshi *et al*, 2004, 2007; Yuji *et al*, 2005; Misawa *et al*, 2006; Ballen *et al*, 2007; Brunstein *et al*, 2007; Komatsu *et al*, 2007; Uchida *et al*, 2008).

First published online 25 August 2009
doi:10.1111/j.1365-2141.2009.07863.x

Engraftment failure is a critical problem that can arise after CBT. The limited doses of infused total nucleated and $CD34^+$ cells contained in umbilical cord blood are thought to influence the rate and kinetics of haematopoietic recovery. In order to overcome engraftment failure, various kinds of strategies, such as multiple unit or *ex-vivo* expanded CBT, and co-infusion of peripheral blood stem cells, have been employed (Shpall *et al*, 2002; Fernandez *et al*, 2003; Barker *et al*, 2005).

Several recent reports have described HPS that arose after autologous and allogeneic HSCT followed by engraftment failure (Sokal *et al*, 1987; Levy *et al*, 1990; Reardon *et al*, 1991; Nagafuji *et al*, 1998; Sato *et al*, 1998; Takahashi *et al*, 1998; Ishikawa *et al*, 2000; Fukuno *et al*, 2001; Abe *et al*, 2002; Tanaka *et al*, 2004, 2007; Kishi *et al*, 2005a; Boelens *et al*, 2006; Ostronoff *et al*, 2006; Ishida *et al*, 2007; Koyama *et al*, 2007). In a reduced-intensity conditioned CBT (RI-CBT) setting, we experienced one patient who failed to achieve engraftment due to HPS following HSCT (HSCT–HPS). Following this case, several similar cases were observed in our institute. We postulated that HPS could play a critical role in engraftment failure after CBT. This report describes the characteristics of 20 patients with HSCT–HPS among 119 who underwent CBT.

Materials and methods

Patients

The study population consisted of 119 adult patients with haematological diseases, who underwent CBT as the first allogeneic HSCT at Toranomon Hospital, Tokyo, Japan between January 2004 and December 2006. All the patients were incurable using conventional approaches, lacked a human leucocyte antigen (HLA)-identical sibling or a suitable unrelated donor from Japan Marrow Donor Program. Most of the patients were considered inappropriate for conventional myeloablative allogeneic HSCT due to being >50 years and/or having organ dysfunction (cardiac ejection fraction <50%, forced expiratory volume 1·0 s % <80%, or serum creatinine > 1·5× upper limit of normal range). Written informed consent was provided by all patients in accordance with the Declaration of Hersinki. The Institutional Review Board of Toranomon Hospital approved the study.

Transplantation procedures

Cord blood units that were serologically matched for ≥4 of six HLA antigens and which contained at least $1{\cdot}8 \times 10^7$ nucleated cells/kg of recipient body weight before freezing were obtained from the cord blood bank at the Japan Cord Blood Bank Network (Nishihira *et al*, 2003). The units were not depleted of T lymphocytes. All patients received purine analogue-based preparative regimens comprising fludarabine phosphate (125–180 mg/m^2), melphalan (80–140 mg/m^2) or busulfan (BU; 8–16 mg/kg) and 0–8 Gy of total body irradiation (TBI), as decided by the treating physician. Graft-versus-host disease (GVHD) prophylaxis comprised a continuous intravenous infusion of either 0·03 mg/kg of tacrolimus (TAC) or 3 mg/kg of ciclosporin (CsA), starting on day-1, except eight patients who received 2 g/d of mycophenolate mofetil (MMF) starting on day-1 in addition to TAC.

Supportive cares

All the patients were treated in reverse isolation in laminar airflow-equipped rooms and received trimethoprim/sulfamethoxazole for *Pneumocystis jirovecii* prophylaxis. Fluoroquinolone and azole and acyclovir were administered to prevent bacterial, fungal and herpes virus infection, respectively. Neutropenic fever was managed according to the guidelines (Hughes *et al*, 2002). Cytomegalovirus pp65 antigenaemia was monitored weekly and preemptive therapy with foscarnet was initiated in the event of a positive result (Matsumura *et al*, 2007; Narimatsu *et al*, 2007a). Haemoglobin and platelet counts were maintained at >70 g/l and 10×10^9/l, respectively. Granulocyte colony-stimulating factor was administered intravenously from day 1 until neutrophil recovery became durable.

Assessment of engraftment, chimaerism, pre-engraftment immune reactions, disease risk and survival

Engraftment was defined as the first of three consecutive days in which white blood cell counts were $>1{\cdot}0 \times 10^9$/l or the absolute neutrophil counts were $>0{\cdot}5 \times 10^9$/l. When the above definition was not met by day 28 without subsequent neutrophil recovery, the patient was considered to have primary engraftment failure. Delayed engraftment was defined as neutrophil engraftment after day 29. Secondary engraftment failure was defined as a decrease in the neutrophil count to $<0{\cdot}5 \times 10^9$/l for three consecutive days after successful engraftment. The date of platelet recovery was defined as the first of seven consecutive days during which the non-transfused platelet count was at least 20×10^9/l.

Chimaerism was assessed using fluorescent *in situ* hybridization (FISH) in sex-mismatched donor–recipient pairs. In sex-matched pairs, chimaerism was assessed using the polymerase chain reaction for variable numbers of tandem repeats with donor cells detected at 10% sensitivity (Thiede *et al*, 1999).

Pre-engraftment immune reactions (PIR) were diagnosed when febrile patients (body temperature ≥38·0°C) developed skin eruption, diarrhoea, jaundice (serum total bilirubin >34·2 μmol/l) or body weight gain of >10% of baseline, with no direct evidence of infection or adverse effects of medication, developing ≥6 d before engraftment (Kishi *et al*, 2005b).

Patients with acute myeloid leukaemia in first or second complete remission (CR) at the time of transplant, with acute lymphoblastic leukaemia in first or second CR, with chronic myeloid leukaemia in the chronic phase, with refractory

anaemia or refractory anaemia with ringed sideroblasts of myelodysplastic syndrome and with non-malignant diseases were defined as being at standard risk. All other patients were defined as being at high risk.

The overall survival (OS) of all of the patients was measured from the date of transplantation to the date of death from any cause.

Definition of haemophagocytic syndrome following haematopoietic stem cell transplantation

We modified the criteria proposed by others for diagnosing HPS after transplantation (Henter *et al*, 1991; Imashuku, 1997; Tsuda, 1997) and selected two major and four minor criteria. A diagnosis of HSCT–HPS required both major criteria, or one major and all four minor criteria. The first major criterion comprised engraftment failure, delayed engraftment, or secondary engraftment failure after HSCT and the second was histopathological evidence of haemophagocytosis. The four minor criteria comprised high grade fever, hepato-splenomegaly, elevated ferritin and elevated serum lactate dehydrogenase (LDH). Although progressive cytopenia has formed the backbone of the previous criteria, we excluded it considering the post-HSCT setting.

Statistical analysis

The cumulative incidences were estimated for neutrophil engraftment and the development of HSCT–HPS (Gooley *et al*, 1999). The probability of OS was estimated from the time of transplantation according to the Kaplan–Meier product limit method and outcomes were compared using the log-rank test. The following patient or transplant characteristics (baseline factors) were analysed using the Cox regression model to determine their impact on the development of HSCT–HPS: patient age, gender (matched or mismatched), blood type (matched or mismatched), disease (lymphoma or not), disease risk (standard or high), preparative regimen (reduced-intensity or myeloablative), GVHD prophylaxis (TAC alone or others), disparity of HLA-A, -B, -DR antigen (one or two mismatched antigens), and numbers of infused nucleated and $CD34^+$ cells. A value of $P < 0{\cdot}05$ was considered statistically significant. All data were statistically analysed using StatView 5.0 and S-Plus 2000 (Mathsoft, Seattle, WA, USA).

Results

Patient's characteristics

Table I summarizes the characteristics of the 119 patients and cord blood grafts. The median age was 55 years (range, 17–69); 103 patients (87%) had high risk diseases. The preparative regimen comprised fludarabine phosphate, melphalan and TBI in 91 patients (76%) and 106 patients (89%) received TAC alone as GVHD prophylaxis. MMF was administered in addition to TAC for eight patients (7%). The median numbers of infused total nucleated and $CD34^+$ cells were $2{\cdot}52 \times 10^7$ (range, 1·85–5·13) and $0{\cdot}766 \times 10^5$ cells/kg (range, 0·110–3·16), respectively. The donor–recipient pairs had serological

Table I. Patients' characteristics and transplantation procedures.

Characteristic	Number
Age (years), median (range)	55 (17–69)
Gender (male/female)	78/41
Primary diseases	
Acute lymphoblastic leukaemia	10
Acute myeloid leukaemia	52
Chronic myeloid leukaemia	5
Adult T-cell leukaemia/lymphoma	11
Myelodysplastic syndrome	6
Malignant lymphoma	32
Aplastic anaemia	1
Chronic idiopathic myelofibrosis	1
Acute leukaemia of ambiguous lineage	1
Preparative regimens	
Flu (125–180 mg/m^2)/Mel (80–140 mg/m^2)/TBI (2–8 Gy)	91
Flu (125–180 mg/m^2)/Mel (80–140 mg/m^2)	7
Flu (125–180 mg/m^2)/BU (8–16 mg/kg)/TBI (4–8 Gy)	14
Flu (150–180 mg/m^2)/BU (8–16 mg/kg)	3
Others	4
GVHD prophylaxis	
CsA alone	5
TAC alone	106
TAC and MMF	8
Cord blood cells	
Number of infused nuclear cells, median (range), $\times 10^7$/kg	2·52 (1·85–5·13)
Number of infused $CD34^+$ cells, median (range), $\times 10^5$/kg	0·766 (0·110–3·16)
Sex match	
Matched	24
Mismatched	95
HLA match	
6/6	2
5/6	14
4/6	103
ABO-blood type match	
Matched	36
Minor mismatched	31
Major mismatched	38
Bidirectional mismatched	14
Disease risk	
Standard/high	16/103

GVHD, graft-*versus*-host disease; BU, busulfan; CsA, ciclosporin; Flu, fludarabine phosphate; Mel, melphalan; MMF, mycophenolate mofetil; TAC, tacrolimus; TBI, total body irradiation; HLA, human leucocyte antigen.

mismatches at two HLA loci, a gender mismatch and an ABO blood-type mismatch in 103 (87%), 95 (80%) and 83 (70%) patients, respectively. Among 103 patients who survived beyond 28 d after CBT, neutrophil engraftment was achieved in 89 of them at a median of day 20 (range, 11–45). The cumulative incidence of neutrophil engraftment at day 60 was 85·6%. Secondary engraftment failure occurred in four of these 89 patients. Eleven patients were diagnosed with 'delayed engraftment' according to our definition. The direct causes of death in 16 patients who died within 28 d of CBT included sepsis (n = 10), haemorrhage (n = 2), relapse of primary disease (n = 2), thrombotic microangiopathy (TMA) (n = 1), and central nervous system complication (n = 1). Chimaerism data was obtained from 111 patients. Chimaerism analysis was performed in 58 patients in the peripheral blood and in 53 patients in the bone marrow. One hundred (90·1%) of them had achieved complete donor chimaerism by day 60. The median length of time required to complete donor chimaerism was 18 d (range, 9–93). Chimaerism was analysed in 10 of 16 patients who died within 28 d of CBT. All except one had complete donor chimaerism before neutrophil engraftment. Seventy-three (61·3%) of the 119 patients developed PIR. By day 100 after CBT, 55 patients had developed bacteraemia at a median of 10 d (range, 3–89 d). Of these 55 patients, 33 developed bacteraemia within 14 d of transplantation. Cytomegarovirus (CMV) was reactivated in 60 patients at a median of 33 d (range, 3–101 d). Ten patients developed histologically confirmed CMV enterocolitis. Eleven patients developed limbic encephalitis caused by human herpes virus 6 (HHV-6) at a median of 20 d of transplantation (range, 13–33 d).

HSCT–HPS patients' characteristics

Table II shows the characteristics of the 20 of 119 patients who had clinical features of HPS according to our diagnostic criteria. The cumulative incidence of HPS after CBT was 16·8% (Fig 1). HPS occurred within 4 weeks of transplantation and the median day of diagnosis was 15 d post-transplant (range, 10–27 d). The 20 patients comprised 13 men and seven women, with a median age of 52 years (range, 23–69 years); 17 patients had high risk disease. None of them had evidence of HPS before transplantation. The preparative regimen comprised fludarabine phosphate, melphalan and TBI for 15 patients and 19 patients received TAC alone as GVHD prophylaxis. MMF was administered in addition to TAC for one patient. The median numbers of infused total nucleated and $CD34^+$ cells were $2{\cdot}40 \times 10^7$ cells/kg (range, 1·98–5·13) and $0{\cdot}52 \times 10^5$ cells/kg (range, 0·18–3·10), respectively. The

Table II. Characteristics of HSCT–HPS patients.

Patient	Age (years)/ gender	Disease	Status	TNC ($\times 10^7$/kg)	$CD34^+$ ($\times 10^5$/kg)	Gender match	HLA match	Blood type match	Preparative regimen	GVHD prophylaxis
117	68/M	ALL	RL1	2·64	0·74	Match	4/6	BD MM	F125/M80/TBI4	TAC
157	38/M	AML	PIF	2·39	0·31	MM	4/6	Minor MM	F125/M80/TBI4	TAC
161	69/M	NHL	RL1	2·54	0·99	Match	4/6	Major MM	F125/M80/TBI4	TAC
164	48/F	ATLL	PR	5·13	3·10	MM	4/6	Minor MM	F125/M80/TBI4	TAC
171	23/M	AML	RL2	2·30	0·52	MM	5/6	Minor MM	F180/B8/TBI8	TAC
181	62/M	AML	CR2	1·94	0·18	MM	4/6	Major MM	F125/M80/TSP	TAC
194	61/M	CML	BC	2·25	1·47	MM	5/6	Match	F125/M80/TBI4	TAC
198	56/F	ATLL	PR	3·99	0·20	MM	4/6	BD MM	F125/B8/TBI4	TAC
208	52/M	NHL	PD	2·41	0·52	MM	4/6	Minor MM	F125/M80/TBI4	TAC
209	52/M	AML/MDS	CR1	2·52	0·58	Match	4/6	Major MM	F125/M80/TBI4	TAC
212	57/M	AML/MDS	NT	2·08	0·57	MM	4/6	Minor MM	F125/M80/TBI4	TAC
215	47/F	NHL	PD	3·16	0·45	MM	4/6	Major MM	F180/B8	TAC
239	50/F	AML/MDS	PIF	2·34	0·31	MM	6/6	Match	F180/M140/TBI4	TAC
240	39/M	AML	RL1	2·62	0·29	MM	4/6	Minor MM	F125/M140/TBI4	TAC
242	33/F	AML	RL1	2·57	0·39	MM	4/6	Minor MM	F125/M160/TBI4	TAC
246	66/M	AML/MDS	PIF	2·37	0·65	MM	4/6	Major MM	F125/M80/TBI4	TAC
274	31/F	NHL	RL pASCT	2·72	0·22	MM	4/6	Match	F180/M140	TAC
278	59/M	AML/MDS	PIF	1·98	0·50	MM	4/6	Major MM	F125/M80/TBI4	TAC
280	40/F	NHL	RL1	2·35	0·90	Match	4/6	Minor MM	F125/M80/TBI4	TAC
282	62/M	AML	CR2	2·05	0·70	Match	4/6	Minor MM	F125/M80/TBI4	TAC/MMF

ALL, acute lymphoblastic leukaemia; AML, acute myeloid leukaemia; AML/MDS, acute myeloid leukaemia with multilineage dysplasia; ATLL, adult T-cell leukaemia/lymphoma; B, oral busulfan, mg/kg; BC, blastic crisis; BD, bidirectional; CML, chronic myeloid leukaemia; CR, complete response; F, fludarabine; GVHD, graft-*versus*-host disease; HLA, human leucocyte antigen; M, melphalan, mg/m^2; MDS, myelodysplastic syndrome; MM, mismatch; MMF, mycophenolate mofetil; NHL, non-Hodgkin lymphoma; NT, not treated; pASCT, post autologous stem-cell transplantation; PD, progressive disease; PIF, primary induction failure; PR, partial response; RL, relapse; TAC, tacrolimus; TBI, total body irradiation; TNC, total nucleated cell count; TSP, tespamine.

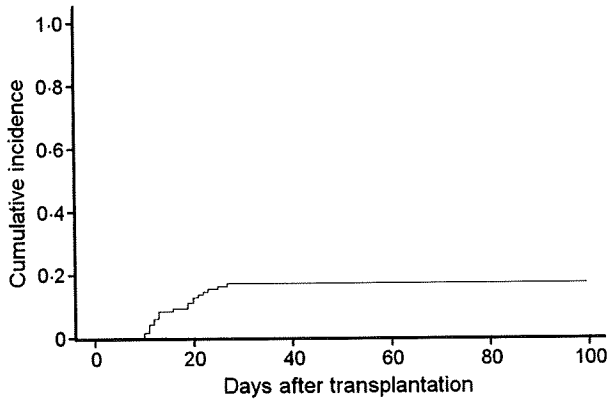

Fig 1. Cumulative incidence of HPS following CBT.

donor–recipient pairs had serological mismatches at two HLA loci, a gender mismatch and an ABO blood type mismatch in 17, 15 and 17 patients, respectively.

Clinical features of HSCT–HPS patients

Table III shows the clinical features and outcome of HSCT–HPS patients. All patients, except for one, presented with high grade fever. Hepatosplenomegaly was found in four patients and 11 had clinical manifestations of PIR. Serum aminotransferases (predominantly aspartate, rather than alanine aminotransferase) and bilirubin were elevated in 12 patients each. None of them had acute hepatic failure. Serum LDH and ferritin levels were elevated in 16 and 19 patients respectively [median value (range) of highest LDH, 340 (65–2444) i/u per litre and ferritin, 9397 (1423–568500) μg/l]. The highest values of serum ferritin by day 30 after CBT significantly differed between patients with and without HPS ($P < 0{\cdot}0094$) (Fig 2). The diagnosis of HPS was confirmed by cytological or pathological assessment of all patients, except for one with extremely elevated serum ferritin who rapidly developed secondary engraftment failure, which was strongly indicative for HSCT–HPS. Bone marrow aspirates from 18 of 19 patients exhibited haemophagocytosis (the remaining one was diagnosed by a bone marrow biopsy post-mortem). This test was performed between day 10 and 27 d after transplantation to determine the cause of delayed neutrophil recovery or to predict the development of HPS. Bone marrow aspiration smear showed very hypocellular marrow with a prominent increase of activated macrophages phagocytosing red cells and myeloid precursors.

Engraftment and chimaerism of HSCT–HPS patients

Of 14 patients with HPS who failed to engraft (primary engraftment failure), eight died within 28 d of CBT. Three patients achieved engraftment after day 29 of CBT (delayed

Table III. Clinical features and outcome of HSCT–HPS patients.

Patient	Engraftment (d)	M in BM (%)	Day of Dx	Chimaerism (% donor)	PIR	Fever	HSM	LDH (i/u per litre)	Ferritin (μg/l)	Intervention	Response
117	Not engrafted	29·0	19	NA	No	Yes	No	65	NA	None	Not engrafted
157	Not engrafted	66·0	19	98·4	Yes	Yes	Yes	1255	1423	CS/CsA	Not engrafted
161	Day 19, sEF	NA*	NA*	NA*	Yes	Yes	No	1372	9397	CS	Not engrafted
164	Day 13, sEF	1·0	25	96·2	No	Yes	Yes	2444	568500	CS/CsA	Engrafted
171	Not engrafted	43·0	27	0·2	No	Yes	No	166	6434	CS	Not engrafted
181	Not engrafted	53·0	12	94·0	No	Yes	Yes	587	18150	CS	Not engrafted
194	Not engrafted	24·0	13	98·8	Yes	Yes	No	664	34200	CS	Not engrafted
198	Not engrafted	17·0	20	94·6	Yes	Yes	No	208	2719	CS	Not engrafted
208	Not engrafted	21·5	13	99·6	Yes	Yes	No	994	18640	CS/VP16	Not engrafted
209	Not engrafted	51·0	12	64·0	No	Yes	No	174	1946	IVIG/second CBT	Engrafted
212	Day 30	30·5	11	63·6	Yes	Yes	NE	261	9339	IVIG	Engrafted
215	Day 33	18·5	21	99·8	Yes	Yes	No	216	9808	CS	Engrafted
239	Day 30	25·0	22	96·4	Yes	Yes	NE	313	5212	CS	Engrafted
240	Not engrafted	15·0	11	99·0	Yes	Yes	NE	268	58824	CS	Not engrafted
242	Not engrafted	10·0	10	96·4	Yes	Yes	No	143	3439	IVIG/second CBT	Engrafted
246	Not engrafted	15·0	21	18·2	No	Yes	No	800	7740	Second CBT	Engrafted
274	Not engrafted	90·0	11	68·4	Yes	Yes	NE	367	20304	Second CBT	Engrafted
278	Not engrafted	34·0	10	99·4	Yes	Yes	No	891	111800	None	Not engrafted
280	Not engrafted	11·5	13	100	No	Yes	Yes	1634	67600	CS/VP16	Not engrafted
282	Day 24, sEF	58·0	20	92·6	No	No	No	276	2464	CS	Not engrafted

BM, bone marrow; CBT, cord blood transplantation; CS, corticosteroid; CsA, ciclosporin; Dx, diagnosis; HSM, hepatosplenomegaly; IVIG, intravenous immunoglobulin; M, macrophage; NA, not available; NE, not evaluated; PIR, pre-engraftment immune reactions; sEF, secondary engraftment failure.

*Haemophagocytosis confirmed by post-mortem bone marrow biopsy.

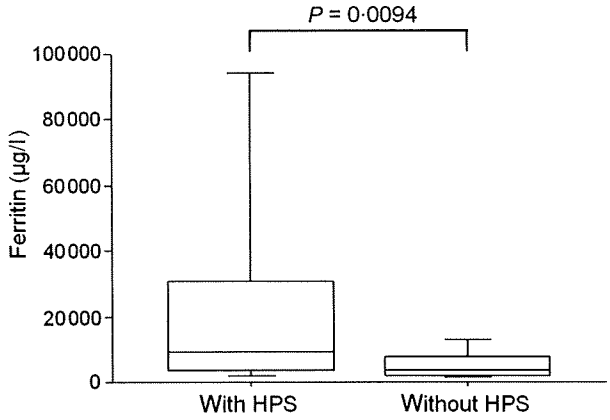

Fig 2. Comparison of highest value of serum ferritin by day 30 of CBT (with *versus* without HPS).

engraftment). Secondary engraftment failure occurred in three patients. Chimaerism data were obtained from 18 out of 20 patients. Donor chimaerism was complete at the time of HPS diagnosis in 13 patients. Three and two patients had donor- and recipient-dominant chimaerism, respectively. An examination of bone marrow clot specimens using XY-FISH method (Ishida *et al*, 2007) confirmed that the activated macrophages in two patients with HPS who achieved complete donor chimaerism (patients 157 and 181; Table II) were donor-derived.

Concomitant clinical conditions of HSCT–HPS patients

Concomitant clinical conditions might be relevant to the development of HPS. Twelve of 20 patients had extant infections, most of which were bacteraemia (n = 10). The pathogens in eight patients were Gram-positive cocci, namely coagulase-negative *Staphylococcus* (n = 5), *Enterococcus faecalis* (n = 2) and *Enterococcus faecium* (n = 1), and Gram-negative rods, *Stenotrophomonous maltophilia* (n = 1) and *Pseudomonous aeruginosa* (n = 1) in two. Three patients were infected with CMV. Two had simultaneous bacteraemia and HHV-6 infection was found in one patient who developed limbic encephalitis. Among eight patients who had no documented infections, five developed transient atypical lymphocytosis soon after transplantation, two had PIR, and the remaining patient developed HPS without any concomitant clinical conditions.

Therapeutic interventions for HSCT–HPS and outcome

Corticosteroid (CS) was administered in 13 of 20 patients to reduce macrophage activation, CsA was administered in addition to CS in two patients and etoposide (VP-16) was also administered in addition to CS in two others. Four patients underwent a second rescue CBT, two of which were after the administration of high-dose intravenous immunoglobulin (IVIG). One patient was treated with IVIG alone. Two patients could not undergo specific treatments due to severe infections and/or severe organ damage. These efforts finally resolved the failed engraftment in eight patients. The prognosis was poor; 17 of 20 patients died (85%) and eight had died by 28 d after CBT. The causes of death were sepsis (n = 7), relapse of primary disease (n = 3), haemorrhage (n = 2), TMA (n = 2), GVHD (n = 2) and central nervous system complication (n = 1). As of December 2007, the median follow-up after CBT for surviving patients was 598 d (range, 26–1426 d). The Kaplan–Meier probability of overall survival at 4 years was 31·4% (95% confidence interval, 20·0–42·8%). The overall survival was significantly poorer for patients with HPS than without HPS (15·0% vs. 35·4%; P = 0·0002, Fig 3).

Risk factors for HSCT–HPS

Univariate and multivariate analysis identified having fewer infused $CD34^+$ cells as a significant risk factor for the development of HPS (P = 0·01 and 0·006 respectively, Table IV). Patients were subdivided into two groups according to the intensity of preparative regimen; those who received 16 mg/kg of BU or 8 Gy of TBI were categorized as 'myeloablative' (n = 18), and the others who received less intensive regimens were classified as 'reduced-intensity' (n = 101). The incidence of HPS was higher in the 'reduced-intensity' group, although it did not reach statistical significance (P = 0·17).

Discussion

This study of clinical manifestations, therapeutic management, outcome and risk factors for HPS after CBT is the largest to date. Our results demonstrated that HPS is an aggressive and devastating complication after CBT that closely correlates with delayed engraftment or failure, resulting in a poor OS. As far as we understand from the English medical literature (Table V), only 23 patients in 16 case reports appear to have developed HPS after autologous (n = 5) and allogeneic (n = 18) HSCT

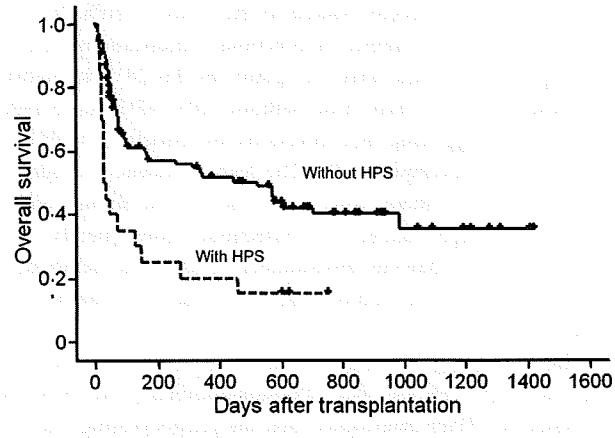

Fig 3. Comparison of overall survival (with *versus* without HPS).

Table IV. Risk factors of HPS development.

Univariate factors		Cumulative incidence	*P* value
Age (<55 vs. ≥55 years)		19·3% vs. 14·5%	0·50
Gender (mismatch *versus* match)		18·3% vs. 11·5%	0·41
Blood type (mismatch *versus* match)		20·8% vs. 8·1%	0·09
Underlying disease (non-lymphoma *versus* lymphoma)		17·1% vs. 16·3%	0·85
Risk of underlying disease (standard *versus* high)		18·8% vs. 16·5%	0·80
Preparative regimen (reduced-intensity *versus* myeloablative)		19·4% vs. 5·6%	0·17
GVHD prophylaxis (TAC alone *versus* others)		18·4% vs. 7·7%	0·35
Disparity of HLA-A, -B, -DR antigen (1 or 0 vs. 2-antigen mismatch)		18·8% vs. 16·5%	0·89
GVH vector (2 vs. 1 or 0-mismatch)		18·4% vs. 12·5%	0·41
HVG vector (1 or 0 vs. 2-antigen mismatch)		21·1% vs. 15·1%	0·53
Number of infused total nucleated cells (<2·52 vs. ≥2·52 × 10^7/kg)		18·6% vs. 15·0%	0·60
Number of infused $CD34^+$ cells (<0·766 vs. ≥0·766 × 10^5/kg)		27·1% vs. 6·8%	0·01
Multivariate factors	**Hazard ratio**	**95% Confidence interval**	***P* value**
Blood type (mismatch *versus* match)	2·80	0·79–9·86	0·11
Preparative regimen (reduced-intensity *versus* myeloablative)	2·76	0·43–17·8	0·29
GVHD prophylaxis (TAC alone *versus* others)	2·71	0·41–17·9	0·30
Number of infused $CD34^+$ cells (<0·766 vs. ≥0·766 × 10^5/kg)	4·48	1·54–13·1	0·006
GVH vector (1 or 0 vs. 2-antigen mismatch)	1·48	0·52–4·21	0·46

GVH, graft-*versus*-host; HVG, host-*versus*-graft.

(Sokal *et al*, 1987; Levy *et al*, 1990; Reardon *et al*, 1991; Nagafuji *et al*, 1998; Sato *et al*, 1998; Takahashi *et al*, 1998; Ishikawa *et al*, 2000; Fukuno *et al*, 2001; Abe *et al*, 2002; Tanaka *et al*, 2004, 2007; Kishi *et al*, 2005a; Boelens *et al*, 2006; Ostronoff *et al*, 2006; Ishida *et al*, 2007; Koyama *et al*, 2007). Among 18 patients who received allogeneic HSCT, reduced-intensity preparative regimens were employed in nine patients and three underwent CBT. Thus, HPS has been considered a rare event after HSCT. The incidence of HPS following CBT in our study, however, was strikingly higher than previous reports have indicated.

Multivariate analyses identified the dose of $CD34^+$ cells as the only statistically significant risk factor. Given that a low dose of $CD34^+$ cells can negatively affect the rate of engraftment and duration to neutrophil recovery, more infectious complications accompanying low $CD34^+$ cell counts might be directly related to the onset of HPS. In our study cohort, the incidence of infectious complications arising during the early phase after transplant (by day 28) was higher in those with HPS than those without HPS (12/20 vs. 37/99; $P = 0·027$), suggesting that infections are associated with the likelihood of developing HPS. The high prevalence of elderly patients and of those with high-risk disease status might explain this high incidence of infections. Consequently, the poor outcome following development of HPS was mainly due to the engraftment failure and following exacerbation of infections.

The intriguing finding of our chimaerism analysis of patients with HPS was that of donor-dominancy in 16 of 18 patients. XY-FISH determined that the phagocytosing macrophages were also of the donor type in the two evaluated patients. These findings indicated that HPS after CBT might be mediated by donor-derived macrophages rather than host-derived, and that engraftment failure is not due to a simple rejection mechanism, but to factors and events that activates donor-derived macrophages and leads to the cascade of HPS. The incidence of HPS may have been underestimated in previous reports, as the reason for graft failure after transplantation had often not been described, especially for graft failure with donor-dominant chimaerism.

The postulated pathophysiology of HPS is that excessive cytokine production from T cells activate macrophages, leading to a substantial loss of haematopoietic cells. Although of great interest, the role of cytokine levels in the precise mechanism of HPS needs further study in the future. We previously described unique early immune reactions after CBT and termed them PIR (pre-engraftment immune reactions), i.e. non-infectious high-grade fever concomitant with eruption, diarrhoea and weight gain, starting on a median of day 9 after CBT (Kishi *et al*, 2005b). In the present study, 61% of the patients developed this syndrome, suggesting that immune cells became activated soon after transplantation. We regarded this syndrome as early onset of acute GVHD, where activated donor T cell secreted various cytokines (Reddy & Ferrara, 2003).

We also recently reported that the degree of HLA mismatch in the graft-*versus*-host direction was inversely associated with engraftment kinetics after RI-CBT (Matsuno *et al*, 2009). Paradoxically to the former notion of graft failure, the degree of HLA mismatch in the host-*versus*-graft direction had no impact on the engraftment kinetics. These findings propose a novel mechanism responsible for

Table V. Occurrence of haemophagocytic syndrome among autologous and allogeneic haematopoietic stem cell transplantation reported in English medical literature.

Ref.	Age (years)/ gender	Disease	Stem cell HLA match	Preparative regimen	GVHD prophylaxis	Day of Dx	Principal cause	Intervention	Response
(A) After autologous haematopoietic stem cell transplantation									
Levy *et al* (1990)	6/F	Wilm tumour	Auto BM	Local RT/Mel/ADM	–	28	ADV-11	IVIG	Not engrafted
Nagafuji *et al* (1998)	52/F	AML	Auto PBSC	BU/VP16/Ara-C	–	25	CMV	CS/IVIG	Not resolved
Takahashi *et al* (1998)	43/F	NHL	Auto PBSC	CY/VP16/MCNU/CBDCA	–	130	Lymphoma	CS/IVIG	Not resolved
Fukuno *et al* (2001)	67/F	NHL	Auto PBSC	CY/VP16/MCNU	–	12	MRSA	CS/CsA	Not engrafted
Ostronoff *et al* (2006)	54/F	MM	Auto PBSC	Mel	–	16	ND	CS/IVIG	Engrafted
(B) After allogeneic haematopoietic stem cell transplantation									
Sokal *et al* (1987)	8/M	FA	ur-BM, 6/6	CY/TBI 4	CsA	300	HSV-1	–	Resolved
Reardon *et al* (1991)	8/F	ALL	r-BM, 6/6	BU/CY	CsA/CS	38	ADV	–	Not resolved
Sato *et al* (1998)	40/F	AML	ur-BM, 6/6	VP16/TBI 12	CsA/sMTX	59	CMV	IVIG/VP16	Not resolved
Ishikawa *et al* (2000)	40/M	AML	r-BM, 6/6	CY/TBI 12	CsA/sMTX	16 (D)	ND	CS	Engrafted
Abe *et al* (2002)	39/M	NHL	r-PBSC, 6/6	TBI 2	CsA/MMF	15 (D)	ND	CS/VP16	Not engrafted
Abe *et al* (2002)	50/F	NHL	r-PBSC, 5/6	TBI 2	CsA/MMF	56 (D)	ND	CS	Not engrafted
Tanaka *et al* (2004)	7/F	AML/MDS	ur-CB, 5/6	CY/TBI 12/Ara-C	CsA/sMTX	20 (D)	MRCNS	CS/second PBSCT	Engrafted
Kishi *et al* (2005a)	30/M	AML	r-PBSC, 5/6	BU/CY	TAC	11	ND	CS	Not resolved
Boelens *et al* (2006)	2/F	HS	r-BM/PBSC, 3/6	Flu/Mel/TSP/ATG	NR	35, sEF (D)	EBV-LPD	CS	Resolved
Ishida *et al* (2007)	2/M	JMML	ur-BM, 6/6	Flu/Mel/BU	TAC/sMTX	39, sEF (R)	NR	IVIG/second CBT	Engrafted
Ishida *et al* (2007)	2/M	JMML	ur-CB, –	Flu/Mel/VP16	TAC	11 (R)	NR	IVIG/VP16	Engrafted
Tanaka *et al* (2007)	54/M	AML	ur-CB, 5/6	CY/TBI 12/Ara-C	CsA/sMTX	33, sEF	NR	CS/second CBT	Engrafted
Koyama *et al* (2007)	9/–	ID	ur-BM, 6/6	Mel/TBI 6/ATG	TAC/sMTX	10	NR	CS/IVIG/VP16	Engrafted
Koyama *et al* (2007)	3/–	AML	r-BM, 4/6	Flu/TBI 12/Ara-C/VP16	TAC/sMTX	10	NR	CS/IVIG	Engrafted
Koyama *et al* (2007)	2/–	ALL	r-PBSC, –	TBI 10/TSP	TAC	8	NR	IVIG/VP16	Not engrafted
Koyama *et al* (2007)	16/–	EBV-LPD	r-PBSC, –	Flu/Mel/ATG	TAC	7	NR	CS/VP16	Not engrafted
Koyama *et al* (2007)	9/–	AML	ur-BM, 6/6	CY/TBI 12/TSP	TAC/sMTX	12	NR	CS/VP16	Engrafted
Koyama *et al* (2007)	3/–	NHL	r-BM, 3/6	TBI 12/VP16/TSP	TAC/sMTX/CS	5	NR	CS/VP16	Engrafted

ADM, adriamycin; ADV, adenovirus; ALL, acute lymphoblastic leukaemia; AML, acute myeloid leukaemia; AML/MDS, acute myeloid leukaemia with multilineage dysplasia; Ara-C, cytosine arabinoside; ATG, anti-thymoglobulin; Auto, autologous; BM, bone marrow; BU, busulfan; CB, cord blood; CBDCA, carboplatin; CMV, cytomegalovirus; CS, corticosteroid; CsA, ciclosporin; CY, cyclophosphamide; Dx, diagnosis; (D), donor-derived; EBV-LPD, Epstein–Barr virus associated lymphoproliferative disorder; F, female; FA, Fanconi anaemia; Flu, fludarabine; HS, Hurler syndrome; HSV, herpes virus; ID, immunodeficiency; IVIG, intravenous immunoglobulin; JMML, juvenile myelomonocytic leukaemia; M, male; MCNU, ranimustine; Mel, melphalan; MM, multiple myeloma; MMF, mycophenolate mofetil; MRCNS, methicillin-resistant coagulase negative *Staphylococcus*; MRSA, methicillin-resistant *Staphylococcus aureus*; ND, not detected; NHL, non-Hodgkin lymphoma; NR, not referred; PBSC, peripheral blood stem cell; r, related; (R), recipient-derived; Ref, reference; RT, radiation therapy; ur, unrelated; sEF, secondary engraftment failure; sMTX, short-term methotrexate; TAC, taclorimus; TBI, total body irradiation; TSP, tespamine; VP16, etoposide.

